

## ALLERGY

# An IL-9–pulmonary macrophage axis defines the allergic lung inflammatory environment

**Yongyao Fu<sup>1</sup>, Jocelyn Wang<sup>1</sup>, Baohua Zhou<sup>2</sup>, Abigail Pajulas<sup>1</sup>, Hongyu Gao<sup>3</sup>, Baskar Ramdas<sup>2</sup>, Byunghee Koh<sup>1</sup>, Benjamin J. Ulrich<sup>1</sup>, Shuangshuang Yang<sup>1</sup>, Reuben Kapur<sup>2</sup>, Jean-Christophe Renaud<sup>4</sup>, Sophie Paczesny<sup>5</sup>, Yunlong Liu<sup>3</sup>, Robert M. Tighe<sup>6</sup>, Paula Licona-Limón<sup>7</sup>, Richard A. Flavell<sup>8</sup>, Shogo Takatsuka<sup>9</sup>, Daisuke Kitamura<sup>9</sup>, Robert S. Tepper<sup>2</sup>, Jie Sun<sup>10</sup>, Mark H. Kaplan<sup>1\*</sup>**

Despite IL-9 functioning as a pleiotropic cytokine in mucosal environments, the IL-9–responsive cell repertoire is still not well defined. Here, we found that IL-9 mediates proallergic activities in the lungs by targeting lung macrophages. IL-9 inhibits alveolar macrophage expansion and promotes recruitment of monocytes that develop into CD11c<sup>+</sup> and CD11c<sup>-</sup> interstitial macrophage populations. Interstitial macrophages were required for IL-9–dependent allergic responses. Mechanistically, IL-9 affected the function of lung macrophages by inducing Arg1 activity. Compared with Arg1-deficient lung macrophages, Arg1-expressing macrophages expressed greater amounts of CCL5. Adoptive transfer of Arg1<sup>+</sup> lung macrophages but not Arg1<sup>-</sup> lung macrophages promoted allergic inflammation that *Il9r*<sup>-/-</sup> mice were protected against. In parallel, the elevated expression of IL-9, IL-9R, Arg1, and CCL5 was correlated with disease in patients with asthma. Thus, our study uncovers an IL-9/macrophage/Arg1 axis as a potential therapeutic target for allergic airway inflammation.

## INTRODUCTION

Macrophages are the most abundant immune cells during homeostasis and a major antigen-presenting cell in the lung that bridges the innate and adaptive immune responses during disease development. Alveolar macrophages (AMs) and interstitial macrophages (IMs) are the two major heterogeneous lung macrophage populations (1). AMs reside in the alveoli, are directly in contact with the environment, and are derived from fetal liver and embryonic monocytes, maintaining a high level of self-proliferation. IMs are located in the interstitium and represent small proportion of lung macrophages during homeostasis (1). Upon challenge, blood monocytes are recruited to the lung, where they can develop into IMs (1, 2). IMs were considered to be a uniform cell population, but recent studies have challenged this paradigm and demonstrated that IMs can be divided into two or three distinct subpopulations (3, 4), including a CX3CR1<sup>+</sup> SiglecF<sup>+</sup> transitional macrophage identified by single-cell RNA sequencing analysis and demonstrated to have profibrotic effects (5). These studies support the idea that lung IMs are a heterogeneous pool; however, our understanding of the heterogeneity of IMs under various disease states and their function during various immune responses is limited.

Interleukin-9 (IL-9) plays a pleiotropic role in disorders including allergic disease and inflammatory bowel disease (6). It activates intracellular signaling by binding to IL-9 receptor (IL-9R) consisting of a unique  $\alpha$  chain (IL-9Ra) and a common  $\gamma$  chain shared with other family cytokine receptors including IL-2 and IL-4 (7, 8). IL-9R is expressed in multiple cell types including activated T cells, type 2 innate lymphoid cells (ILC2s), memory B cells, and mast cells (6, 9–15). Numerous studies report that IL-9/IL-9R signaling can promote allergic inflammation characterized by the induction of chemokines and recruitment of eosinophils (16–18). Asthmatic patients also expressed high amounts of *IL9* and *IL9R* (16, 17, 19). IL-9 enhances allergic responses by directly regulating mast cell function and also indirectly affecting other cells such as eosinophils, B cells, and epithelial cells (6, 15). Nonetheless, the entire IL-9–responsive cell repertoire is still unclear.

As one of the most abundant immune cells in the lung, macrophages are key players in allergic responses. Previous studies showed that IL-9 affects the oxidative burst of human blood monocytes and AMs, but little is known about how IL-9 affects the heterogeneity of lung macrophages and how that function might be linked to disease development (20, 21). In this study, we defined a comprehensive IL-9–responsive repertoire in allergic lung environment. We found that there are three distinct IL-9–responsive lung macrophage populations in the allergic lung. IL-9 inhibits the proliferation of AMs, promotes monocyte migration to the lung, and expands the IM population. The induction of CD11c<sup>+</sup> IM is mediated by IL-9 signaling in the context of allergic inflammation. Macrophages are the key drivers of IL-9–mediated immune response, with IL-9 regulating macrophage function by increasing Arg1 expression and arginase activity. Compared with Arg1<sup>-</sup> macrophages, Arg1<sup>+</sup> macrophages express greater CCL5, a chemokine that promotes allergic airway inflammation through recruitment of eosinophils (22). Adoptive transfer of Arg1-expressing macrophages restores allergic inflammation in *Il9r*<sup>-/-</sup> mice. Evidence of the IL-9/macrophage/Arg1 axis was also found in patients with asthma. Thus, our study advances the current understanding of IL-9–mediated allergic response and

Copyright © 2022  
The Authors, some  
rights reserved;  
exclusive licensee  
American Association  
for the Advancement  
of Science. No claim  
to original U.S.  
Government Works

<sup>1</sup>Department of Microbiology and Immunology, Indiana University School of Medicine, Indianapolis, IN 46202, USA. <sup>2</sup>Department of Pediatrics and Herman B Wells Center for Pediatric Research, Indiana University School of Medicine, Indianapolis, IN 46202, USA. <sup>3</sup>Department of Medical and Molecular Genetics, Indiana University School of Medicine, Indianapolis, IN 46202, USA. <sup>4</sup>Ludwig Institute for Cancer Research, Experimental Medicine Unit, Université Catholique de Louvain, Brussels 1200, Belgium. <sup>5</sup>Department of Microbiology and Immunology, Medical University of South Carolina, 171 Ashley Avenue, Charleston, SC 29425, USA. <sup>6</sup>Division of Pulmonary, Allergy, and Critical Care Medicine, Duke University Medical Center, Durham, NC 27710, USA. <sup>7</sup>Departamento de Biología Celular y del Desarrollo, Instituto de Fisiología Celular, Universidad Nacional Autónoma de México, 04510 Mexico City, Mexico. <sup>8</sup>Department of Immunobiology, Yale University School of Medicine, New Haven, CT 06510, USA. <sup>9</sup>Division of Molecular Biology, Research Institute for Biomedical Sciences (RIBS), Tokyo University of Science, Noda, Japan. <sup>10</sup>Department of Medicine, Mayo Clinic, Rochester, MN 55905, USA.  
\*Corresponding author. Email: mkaplan2@iupui.edu

provides a rationale for targeting IL-9-responsive lung macrophages in therapeutic development.

## RESULTS

### Deficiency of IL-9R inhibits allergic airway inflammation

Asthmatic patients express high amounts of IL-9 and IL-9R (16, 17, 19), and among all organs, the lung has one of the highest *IL9R* expression patterns in healthy donors (fig. S1A). Although IL-9 can affect multiple cell types, the cells that directly respond to IL-9 in the lung are not well studied. To begin to explore this question in the context of a proallergic environment, we used a chronic house dust mite (HDM) challenge model (Fig. 1A). Compared with wild-type (WT) mice, *Il9r<sup>-/-</sup>* mice showed less lung inflammation demonstrated by decreased airway resistance (Fig. 1B), cellular infiltration of the lung (Fig. 1C and fig. S1B), total bronchoalveolar lavage fluid (BALF) cell numbers (Fig. 1D), BALF eosinophils (Fig. 1E), lung eosinophils (Fig. 1F), HDM-specific immunoglobulin E (IgE) production (Fig. 1G), and mucus production (Fig. 1, H and I). In our model, IL-9R deficiency inhibited accumulation of mast cells (Fig. 1, J and K, and fig. S1C), a well-known IL-9-responsive cell, and serum MCPT1 production (Fig. 1L). Serum mast cell protease-1 (MCPT1) was undetectable in phosphate-buffered saline (PBS)-challenged mice (Fig. 1L). The loss of IL-9R did not affect the numbers of T cells, B cells, or cytokine production from CD4<sup>+</sup> T cells (fig. S1, D and E). These results show that IL-9 signaling is critical in a chronic allergic lung inflammation model *in vivo*. Consistent with published reports (6, 15), CD4<sup>+</sup> T cells were major IL-9 producers in the chronic allergic response (Fig. 1M and fig. S1F).

To broadly determine the contribution of hematopoietic and nonhematopoietic cells to IL-9-dependent allergic responses, a bone marrow (BM) chimera experiment was performed (Fig. 1N). Compared with the WT BM to WT recipient chimera group (WT → WT), the overall inflammation in both WT → *Il9r<sup>-/-</sup>* and *Il9r<sup>-/-</sup>* → WT chimeras was diminished (Fig. 1, O to S), indicating that both hematopoietic cells and nonhematopoietic cells responded to IL-9 and contributed to allergic inflammation. However, there was a greater impact of loss of IL-9R in hematopoietic cells (Fig. 1, O to S), suggesting a stronger effect of IL-9/IL-9R signaling in hematopoietic cells during an allergic response.

### Lung macrophages are key IL-9 responders in allergic pulmonary inflammation

We further observed lung F4/80<sup>+</sup> CD206<sup>+</sup> macrophages decreased in the *Il9r<sup>-/-</sup>* group compared with the WT group (fig. S2A). To better understand how different pulmonary macrophage populations respond to IL-9 during allergic responses, we examined AMs and IMs separately to track their activities. Total lung macrophages were identified as CD64<sup>+</sup> MerTK<sup>+</sup> cells (Fig. 2A). AMs and IMs were distinguished by SiglecF and CD11c expression (Fig. 2A). In naïve mice, AMs were the major pulmonary macrophage, whereas IMs composed a small proportion of the total lung macrophages (Fig. 2A). During the allergic response, lung macrophages were present in three populations: AMs, CD11c<sup>-</sup> IMs, and a third population that we termed CD11c<sup>+</sup> IMs, which is supported in subsequent analyses (Fig. 2, A and B). Among them, the CD11c<sup>+</sup> IM population expanded considerably after HDM challenge (Fig. 2, A and B). We did not observe a population of CX3CR1<sup>hi</sup> CD11c<sup>+</sup> SiglecF<sup>-</sup> cells as previously noted in fibrosis models (fig. S2B) (23–25). During

development of allergic inflammation, the loss of *Il9* or *Il9r* resulted in greater maintenance of the AM population and the reduced accumulation of CD11c<sup>-</sup> and CD11c<sup>+</sup> IMs (Fig. 2, A and B, and fig. S2C). Using a mixed BM chimera approach to generating a model with WT and *Il9r<sup>-/-</sup>* cells in a uniform allergic inflammation (fig. S2D), we defined intrinsic effects of IL-9R loss. *Il9r<sup>-/-</sup>* BM cells had a decreased propensity to become IMs; most AMs in the BAL have recipient mouse origin, and there was no significant difference in monocyte chimerism (Fig. 2C and fig. S2, E and F). To test whether these observations are consistent in other allergen-induced allergic disease model, we performed similar experiments with *Aspergillus fumigatus* (ASP)-induced allergic disease model. Consistent with results from the HDM model, IL-9 signaling inhibited AM and promoted CD11c<sup>-</sup> and CD11c<sup>+</sup> IMs (fig. S2G). Together, these data demonstrated that lung macrophage populations have discernable changes in response to IL-9 during allergic lung disease.

To further define whether lung macrophages directly responded to IL-9, we assessed IL-9R expression on lung cell populations (26). In PBS-treated mice, mast cells, basophils, dendritic cells (DCs), and AMs are the major IL-9R<sup>+</sup> cells (Fig. 2D). During chronic allergic challenge, macrophages occupied an increased proportion of IL-9R<sup>+</sup> cells (Fig. 2D). Moreover, macrophages expressed greater IL-9R than other populations (Fig. 2, E and F, and fig. S2H). To assess whether IL-9 is sufficient to control the redistribution of lung macrophages, IL-9 was intranasally administered to naïve mice for 3 days (Fig. 2G). Consistent with the results in allergic models, intranasal injection of IL-9 led to the redistribution of lung macrophages and increased mast cell numbers, but IL-9 alone did not alter IL-9Rα expression (Fig. 2H and fig. S2I). IL-9 injection failed to alter type 2 cytokine expression in CD4<sup>+</sup> T cells (fig. S2J). Thus, macrophages are a prominent IL-9-responsive cell type during allergic lung inflammation.

Because we demonstrated that lung macrophages respond to IL-9 in allergic inflammation with altered dynamics, we next defined whether this is an IL-9-specific effect. Blocking antibodies against IL-9 or another type 2 cytokine, IL-13, were given to mice for the last 2 weeks of HDM challenges (Fig. 2I). Airway resistance was decreased in mice receiving anti-IL-9 treatment (fig. S2K). Blocking IL-9 signaling increased AMs and inhibited the two IM populations, similar to the pattern observed in *Il9r<sup>-/-</sup>* mice (Fig. 2J and fig. S2L). In contrast, anti-IL-13 antibody failed to alter the lung macrophage populations (Fig. 2K and fig. S2M). Blocking IL-9 or IL-13 did not significantly affect reciprocal cytokine or other type 2 cytokine production in the lung (fig. S2, N to P). We further examined whether IL-9 alters macrophage populations by regulating IL-4R signaling. IL-4R expression in lung macrophages was not affected by IL-9 treatment in naïve mice or IL-9R deficiency in the HDM model (fig. S2, Q and R). *Il4<sup>-/-</sup>* mice demonstrated decreased BAL total cell number (fig. S2S) but comparable IL-9 detected in the BALF of WT mice and *Il4<sup>-/-</sup>* mice (fig. S2T). In contrast to observations in *Il9/Il9r*-deficient mice or with blocking IL-9, IL-4R deficiency resulted in increases of both AMs and CD11c<sup>-</sup> IMs (fig. S2U), whereas CD11c<sup>+</sup> IMs were increased in *Il4<sup>-/-</sup>* mice receiving anti-IL-13 treatment (fig. S2U). Together, these results suggest that IL-9 is distinct among type 2 cytokines in a broad scope of altering macrophage responses and that blocking IL-9 at a late stage in the allergen challenge protocol results in similar changes to the macrophage populations as germline deletion of *Il9* or *Il9r*.

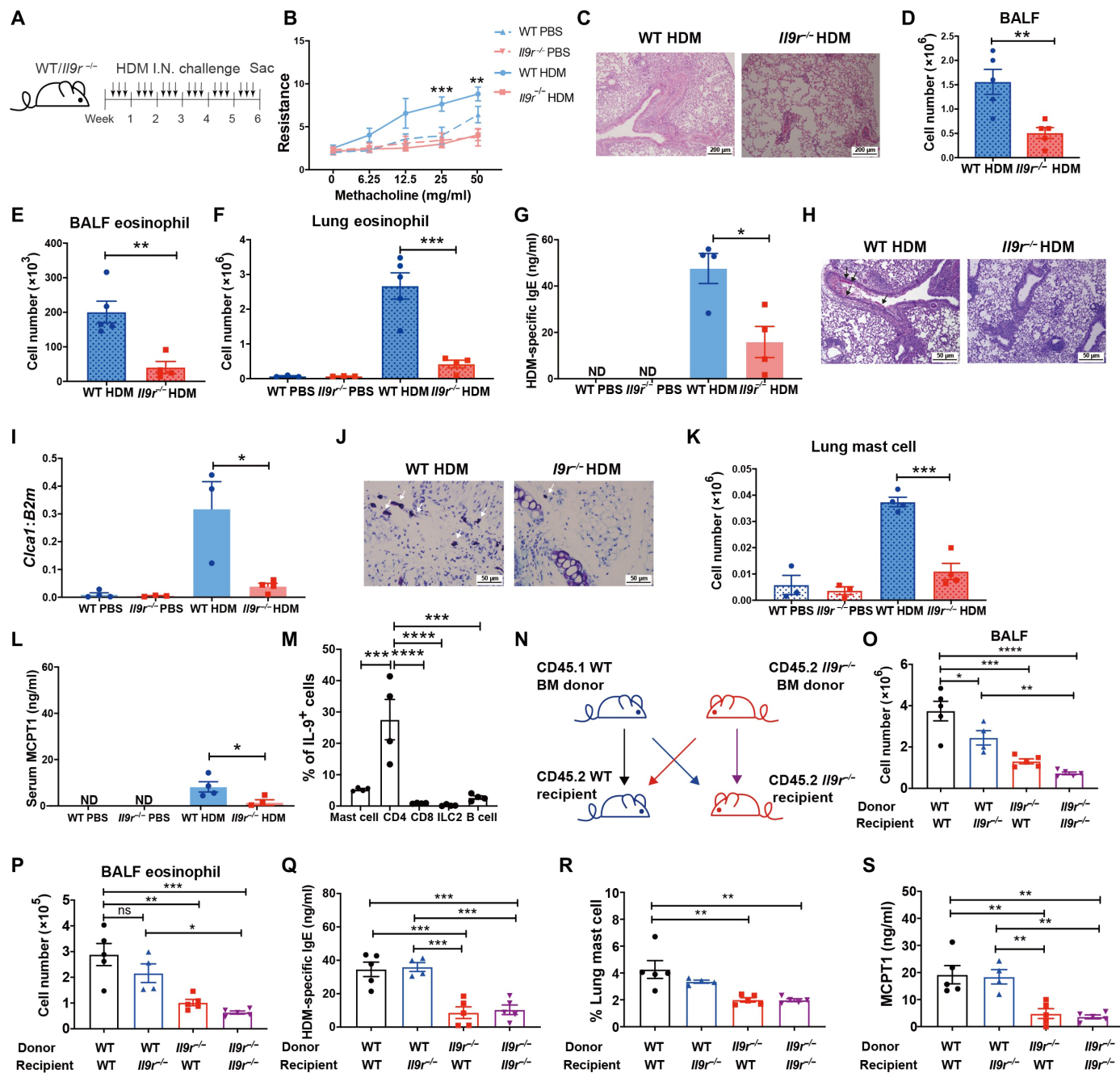
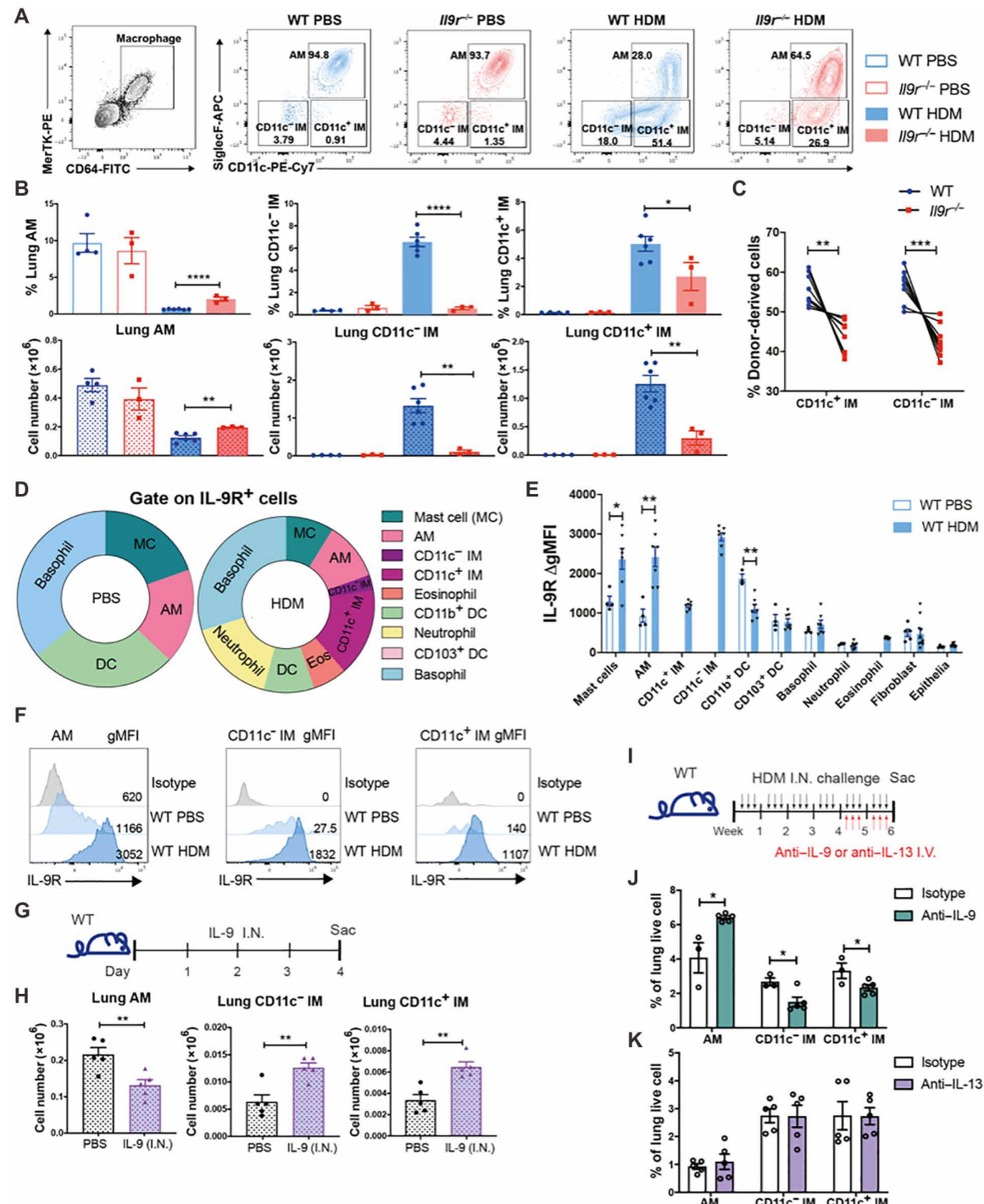


**Fig. 1. Deficiency of IL-9R inhibits allergic airway inflammation.** (A) Schematic of HDM extract-induced airway inflammation model. All measurements, unless indicated, are at the end of week 6. (B) Airway resistance was measured in response to methacholine challenge 1 day after the last HDM treatment ( $n = 3$  to 4 per group). (C) Lung section with H&E staining. (D and E) BALF total cell number and BALF eosinophil number were analyzed ( $n = 4$  to 5 per group). (F) Lung eosinophils were analyzed by flow cytometry ( $n = 3$  to 5 per group). (G) Serum HDM-specific IgE level was analyzed by ELISA ( $n = 4$  per group). (H) Lung section with PAS staining; arrows showed mucus production. (I) Lung Ccl4 mRNA expression was analyzed ( $n = 3$  to 4 per group). (J) Trachea section with toluidine blue staining; arrows show mast cells. (K) Lung mast cells were analyzed by flow cytometry ( $n = 3$  to 4 per group). (L) Serum MCPT1 expression was analyzed by ELISA ( $n = 3$  to 4 per group). (M) IL-9<sup>+</sup> cells were analyzed in HDM-treated IL-9 reporter (infer) mice ( $n = 3$  to 8). (N to S) WT or IL-9r<sup>-/-</sup> BM cells were transferred to lethally irradiated WT or IL-9r<sup>-/-</sup> mice. After reconstitution, the recipient mice were challenged with HDM as shown in (A). BALF total cell number (O), BALF eosinophils (P), serum HDM-specific IgE (Q), lung mast cells (R), and serum MCPT1 level (S) were analyzed ( $n = 4$  to 5). Data are presented as means  $\pm$  SEM from two independent experiments. Unpaired two-tailed Student's *t* test was used for comparison to generate *P* values in (D) to (G), (I), (K), and (L). One-way ANOVA with Tukey's multiple comparisons was used to generate *P* values in (M) and (O) to (S). Two-way ANOVA with Sidak's multiple comparisons was used to generate *P* values in (B). ns,  $P > 0.05$ ; \* $P < 0.05$ , \*\* $P < 0.01$ , \*\*\* $P < 0.001$ , and \*\*\*\* $P < 0.0001$ . ND, undetectable. See also fig. S1. I.N., intranasal.

**Fig. 2. Lung macrophages are key IL-9 responders in allergic response.** Mice were intranasally treated with HDM three times a week for 6 weeks. (A and B) Flow cytometry analysis of lung macrophages ( $n=3$  for WT PBS and  $\text{IL9}^{-/-}$  PBS group;  $n=6$  for WT HDM group;  $n=3$  for  $\text{IL9}^{-/-}$  HDM group). (C) WT (CD45.1) and  $\text{IL9}^{-/-}$  mice (CD45.2) BM cells were mixed in 1:1 ratio and transferred to lethally irradiated recipient mice (CD45.1<sup>+</sup>CD45.2<sup>+</sup> mice). After reconstitution, chimeric mice were treated with HDM; lung macrophages from donor cells were analyzed by flow cytometry ( $n=9$ ). (D to F) Lung cells from PBS- or HDM-treated mice were stained with IL-9R and other surface markers for analysis by flow cytometry. (D) Pie chart analysis of IL-9R<sup>+</sup> cells. (E) Fluorescence intensity of IL-9R among various populations was analyzed.  $\Delta gMFI$  is the geometric mean fluorescence intensity (gMFI) of each population minus the gMFI of isotype controls in that population; there were too few IMs for analysis in PBS-treated mice ( $n=4$  to 7). (F) Histogram of IL-9R in lung macrophage populations. (G and H) Mice were intranasally treated with IL-9 for 3 days (G). (H) Lung macrophages were analyzed by flow cytometry ( $n=5$  per group). (I to K) Mice were treated with HDM for 6 weeks; anti-IL-9, anti-IL-13, or isotype-matched control antibodies were intravenously injected every other day during the last 2 weeks (I). (J and K) Lung macrophages were analyzed by flow cytometry ( $n=3$  to 5). Data are presented as means  $\pm$  SEM from three independent experiments. Unpaired two-tailed Student's *t* test was used for comparison to generate *P* values in (B), (E), (H), and (J). Paired two-tailed *t* tests were used to generate *P* values in (C). \**P* < 0.05, \*\**P* < 0.01, \*\*\**P* < 0.001, and \*\*\*\**P* < 0.0001. See also fig. S2. PE, phycoerythrin. FITC, fluorescein isothiocyanate. APC, allophycocyanin. Cy7, cyanine 7. I.V., intravenously.



### Heterogeneity of pulmonary macrophages and blood monocytes in allergic inflammation

To better define the heterogeneity of pulmonary macrophages upon allergic response, a cellular indexing of transcriptomes and epitopes by sequencing (CITE-seq) with cell hashing experiment was performed. CD64<sup>+</sup> MerTK<sup>+</sup> total lung macrophages and CD11c<sup>+</sup> blood monocytes were sorted from HDM-challenged mice and further

labeled by hashtag oligonucleotide (HTO) antibodies separately. Lung macrophages were stained with antibody-derived tag (ADT) antibodies against CD11c and SiglecF. Lung macrophages and blood monocytes were pooled for analysis with the 10X Genomics Chromium platform (Fig. 3A). Twenty-three clusters were identified from the transcriptome data and visualized by uniform manifold approximation and projection (UMAP) projection (Fig. 3B and

fig. S3A). As defined by HTO labeling of sorted cells, 6 clusters were blood monocytes and 14 clusters were lung macrophages. Some clusters were either dead cells or nonmonocytes/macrophages and were excluded from further analysis (Fig. 3, B and C, and fig. S3A). On the basis of the ADT-defined protein expression profiles and standard cell-identifying gene profiles, we clustered cells as AM, CD11c<sup>-</sup> IM, and CD11c<sup>+</sup> IM (Fig. 3, D and E, and fig. S3B). Several small clusters were ADT-SiglecF<sup>+</sup> but did not have *SiglecF* mRNA and were excluded from analysis.

To further identify the relationship among these clusters, a pseudo-time analysis was performed using CCR2<sup>+</sup> monocytes as the root cell type. We found that CD11c<sup>-</sup> IMs were most closely related to blood monocytes, and AMs shared the least similarity with either CD11c<sup>-</sup> IMs or blood monocytes (Fig. 3F and fig. S3C). Pseudo-time relationships were not altered among cells from *Il9r*<sup>-/-</sup> mice, suggesting that IL-9 affects effector recruitment and/or function but not differentiation (fig. S3C). Consistent with the gene expression profile, the CD11c<sup>+</sup> IMs were more related to blood monocytes and CD11c<sup>-</sup> IMs than AMs (Fig. 3F). CD11c<sup>+</sup> IMs also shared similar morphology with CD11c<sup>-</sup> IMs. Both populations displayed vacuoles in their cytoplasm and nucleus, whereas AMs demonstrated more regular round- or oval-shaped nuclei (Fig. 3G). Hence, we defined this population as CD11c<sup>+</sup> IMs. Although various pulmonary macrophage populations shared some common transcriptional profiles, they also exhibited distinct gene expression patterns (Fig. 3, H to J, and fig. S3D). Moreover, even within each population, transcriptional heterogeneity further defined subsets of cells (Fig. 3J). *Nos2* and *Folr2* are exclusively expressed in CD11c<sup>+</sup> IM clusters (Fig. 3I and fig. S3E). *Cd72* is preferentially expressed in CD11c<sup>-</sup> IMs (fig. S3E). Blood monocytes shared some common markers with IMs including *Tmem176a* and *Tmem176b* (fig. S3G) and also expressed unique genes such as *Trem14* (fig. S3E). The loss of *Il9r* caused alterations in gene expression in both blood monocyte and lung macrophage populations (Fig. 3, K and L, and fig. S3, F and G). IL-9 signaling significantly promoted chemokine expression in macrophage populations (Fig. 3L and fig. S3, F and G). Thus, lung macrophages not only act as IL-9 responders but also potentially contribute to the IL-9-dependent allergic response.

### Lung macrophages amplify IL-9-mediated allergic lung inflammation

To further dissect whether the altered lung macrophage dynamics are a critical component in the development of the allergic response, we first tested whether depleting macrophages would affect allergic airway inflammation. We depleted macrophages in the airway or IMs and circulating monocytes by administering clodronate intranasally or intravenously, respectively (Fig. 4A). Consistent with previous studies, intranasal clodronate injection primarily depleted the AMs without affecting the CD11c<sup>-</sup> IMs (fig. S4, A and B) (27, 28). This treatment did not alter the CD11c<sup>+</sup> IMs (fig. S4B), indicating that the majority of this population does not reside in the airway. Intravenous injection of clodronate successfully depleted blood monocytes and CD11c<sup>-</sup> IMs, but not the AM population (Fig. 4B and fig. S4, C and D). It significantly depleted the CD11c<sup>+</sup> IMs, further supporting that they are residing in the tissue (Fig. 4, B and C, and fig. S4E). WT mice developed reduced lung inflammation similar to *Il9r*<sup>-/-</sup> mice after depletion of monocytes and IMs (Fig. 4, D to F, and fig. S4, F to H), which supports the possibility that blood

monocytes and IMs are required for the development of allergic airway inflammation.

Because the clodronate injection might affect other cell populations, such as monocytes and DCs (fig. S4, C and I), we further defined the functional contribution of the macrophage populations by an adoptive transfer experiment (Fig. 4G). Intranasal adoptive transfer of WT CD11c<sup>-</sup> IMs or CD11c<sup>+</sup> IMs increased airway resistance and lung eosinophil infiltration in *Il9r*<sup>-/-</sup> mice (Fig. 4, H and I). Donor cells were successfully detected in the lung interstitium (Fig. 4J) and fig. S4, J and K), and percentages of DCs were not affected by treatment (fig. S4L). Donor DCs were not detected in mediastinal lymph node (MLN) (fig. S4M). Compared with WT mice, the *Il9r*<sup>-/-</sup> mice that received PBS showed much smaller MLN and transferred AMs did not affect the size of the lymph node (Fig. 4K). However, transfer of either CD11c<sup>-</sup> IMs or CD11c<sup>+</sup> IMs resulted in enlarged MLN to a size comparable with WT mice (Fig. 4K). Mice that received CD11c<sup>+</sup> IMs had substantially larger lymph nodes than the WT mice (Fig. 4K). This was consistent with increased total cell numbers in the MLN (Fig. 4L). Collectively, these findings suggest that lung macrophages, particularly CD11c<sup>+</sup> IMs and CD11c<sup>-</sup> IMs, contribute to IL-9-induced allergic airway disease.

### IL-9 enhances allergic inflammation via recruiting monocytes

To further explore the underlying mechanisms on how IL-9 alters the subpopulations of lung macrophages, we examined the proliferation and cell death of macrophages during the allergic response. Deficiency of *Il9r* increased the proliferation of AMs indicated by a higher amount of Ki67 but did not affect the rate of cell death (fig. S5, A and B). Both WT and *Il9r*<sup>-/-</sup> IMs showed similar capacity for proliferation and cell death, suggesting that other mechanisms were involved in the regulation of IMs by IL-9 (fig. S5, A and B). The efferocytosis capacity of lung macrophages was not affected by the loss of *Il9r* (fig. S5C). Because monocytes are a major source of increased IM in inflammatory environments (2), we hypothesized that IL-9 might affect monocyte recruitment to the lung. Compared with WT mice, the *Il9r*<sup>-/-</sup> mice treated with HDM retained more monocytes in the blood and BM (Fig. 5, A and B). However, IL-9R expression was positively correlated with CCR2 expression, a key chemokine receptor required for classical monocyte migration (Fig. 5, C and D). These data suggested that IL-9 might regulate classical monocyte migration to the lung via CCR2. To directly test this, we performed a migration assay, in which IL-9 and/or CCL2 were added to the lower chamber of a Transwell and BM-derived monocytes that were placed in the upper chamber before cells were allowed to migrate for 3 hours. IL-9 exclusively promoted monocyte migration in the presence of CCL2 (Fig. 5E). Human monocytes from healthy donors also expressed IL-9R, which is consistent with previous studies (Fig. 5F) (21). IL-9 enhanced CCL2-stimulated human peripheral blood mononuclear cell (PBMC)-derived monocyte migration, which likely results from the up-regulation of CCR2 after IL-9 treatment (Fig. 5, G and H). In parallel, we observed that peripheral blood CD14<sup>+</sup> monocytes from children diagnosed with asthma showed increased IL-9R expression compared with monocytes from children that are atopic but did not have physician-diagnosed asthma (Fig. 5I) (29–31). Together, these results suggest that IL-9 promotes the capacity of classical monocytes to migrate to the allergic lung.

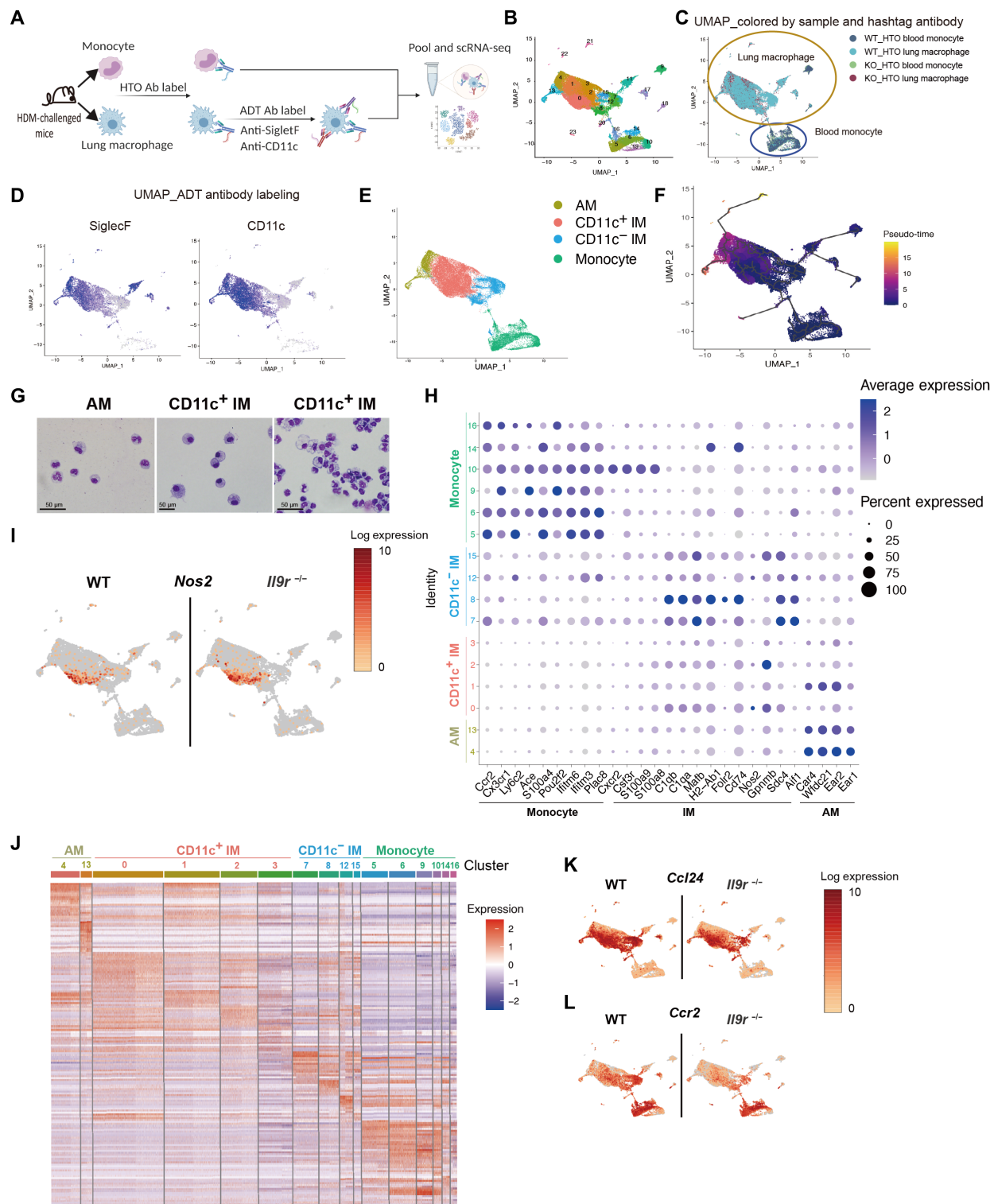
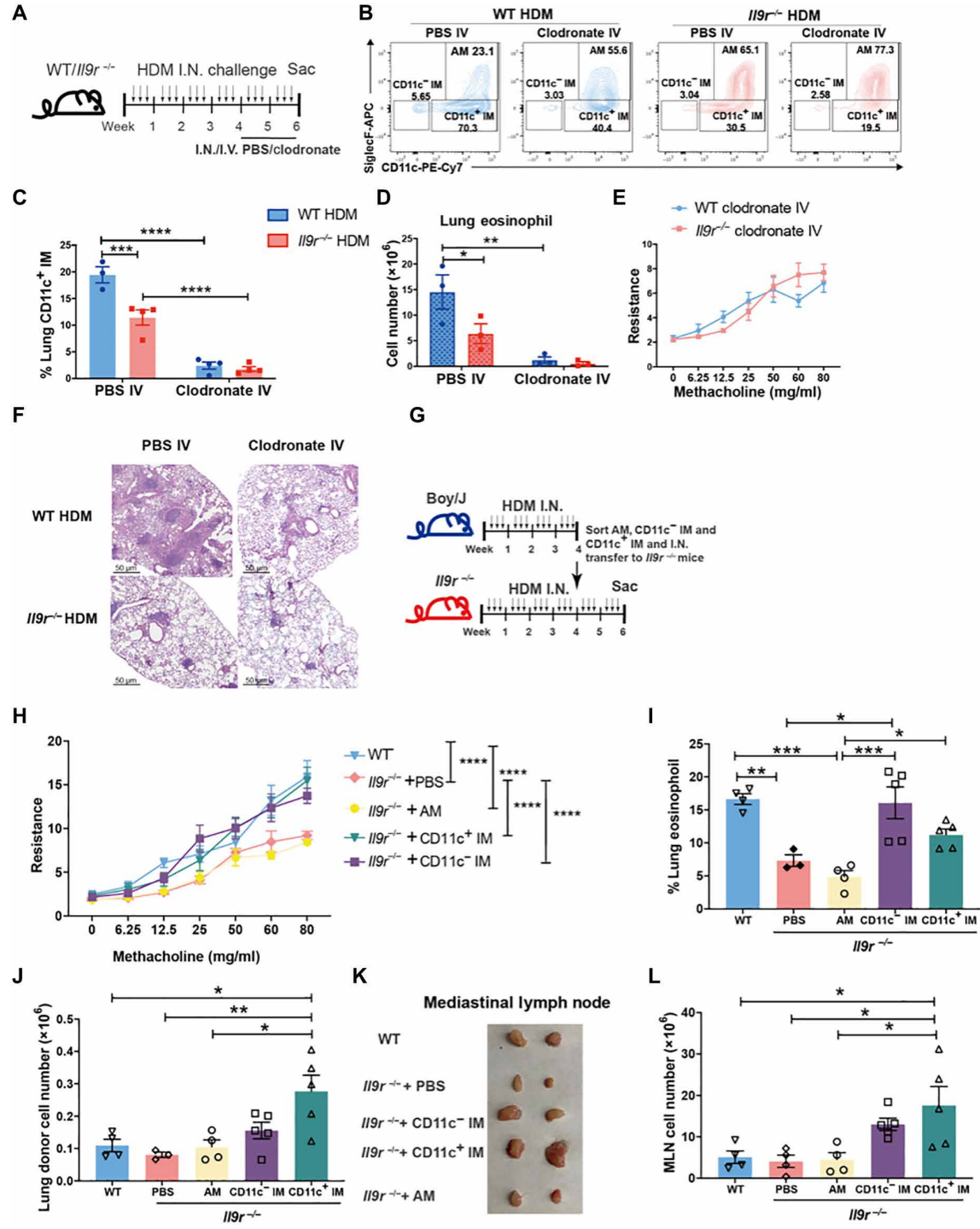


**Fig. 3. Heterogeneity of pulmonary macrophages and blood monocytes in allergic inflammation.** (A to G) CITE-seq combined with cell hashing analysis for blood monocytes and lung macrophages from HDM-challenged mice; 15 mice were pooled per group before FACS sorting (A). (B) UMAP showing clusters based on gene expression. (C) UMAP based on cell hashing antibodies. (D) UMAP based on ADT antibodies. (E) Annotation of the lung macrophages within the UMAP based on both transcriptome and surface proteome. (F) Pseudo-time analysis using CCR2<sup>+</sup> blood monocytes as the root cell type. (G) Lung macrophages were sorted from HDM-treated mice, and morphology was analyzed by cytopsin. (H) Dot plot showing the gene expression in different clusters. The numbers on the y axis are the cluster numbers shown in (B). (I) UMAP showing Nos2 expression. (J) Heatmap showing differentially expressed genes in different clusters. The numbers on the top are the cluster numbers shown in (B). (K and L) UMAP showing the gene expression of the indicated genes. See also fig. S3. Ab, antibody; scRNA-seq, single-cell RNA sequencing.

**Fig. 4. Lung macrophages amplify IL-9-mediated allergic lung inflammation.** (A) Mice were intranasally treated with HDM three times a week for 6 weeks. Clodronate was intranasally or intravenously injected to the mice every other day for the last 2 weeks of the HDM model. (B to F) Mice were treated as described in (A). Lung macrophages (B and C) and eosinophils (D) were analyzed by flow cytometry from lavaged lung. Dot plots indicate the percentage of the total lung macrophage populations. Bar graphs quantify live lung macrophage populations. (E) Airway resistance was measured in response to methacholine challenge 1 day after the last dose of HDM treatment. (F) H&E staining of lung sections ( $n=3$  to 4 per group). (G to L) Boy/J and  $\text{II}9r^{-/-}$  mice were treated with HDM three times a week for 4 weeks. Macrophage populations were sorted from Boy/J mice 1 day after the last HDM treatment and intranasally transferred to  $\text{II}9r^{-/-}$  mice, followed by HDM challenge every other day for another 2 weeks (G). (H) Airway resistance was measured in response to methacholine challenge 1 day after the last HDM treatment at the end of week 6. Statistical differences are indicated between groups in the panel key for clarity. Lung eosinophils (I) and lung donor cells (J) were analyzed by flow. MLN size (K) and cell numbers (L) were analyzed ( $n=3$  to 5 per group). Data are presented as means  $\pm$  SEM from two independent experiments. One-way ANOVA with Tukey's correction for multiple comparisons was used to generate  $P$  values in (I), (J), and (L). Two-way ANOVA with Sidak's multiple comparisons was used to generate  $P$  values in (C) and (D). Two-way ANOVA with Tukey's multiple comparisons was used to generate  $P$  values in (H) to compare group effect using the mean of every group. \* $P < 0.05$ , \*\* $P < 0.01$ , \*\*\* $P < 0.001$ , and \*\*\*\* $P < 0.0001$ . See also fig. S4.

Because the results above supported the idea that IL-9 promotes CCR2-dependent monocyte migration, we tested whether CCR2<sup>+</sup> monocytes were required for the accumulation of CD11c<sup>-</sup> and CD11c<sup>+</sup> IMs. After administration of a CCR2 inhibitor to mice in the HDM model (Fig. 5J), there were increased BM monocytes and reduced lung monocytes, compared with control mice (Fig. 5, K and L, and fig. S5D). This confirmed that the inhibitor successfully arrested



the monocytes in the BM. Furthermore, the inhibitor significantly reduced CD11c<sup>-</sup> and CD11c<sup>+</sup> IMs but had no impact on AMs (Fig. 5M and fig. S5E), supporting the hypothesis that CD11c<sup>-</sup> and CD11c<sup>+</sup> IM accumulation in the lung was dependent on CCR2<sup>+</sup> monocytes. To further confirm this, we isolated BM monocytes from HDM-challenged mice and transferred them to WT CD45.1 recipient mice. IL-9 and HDM were given to the recipient mice for

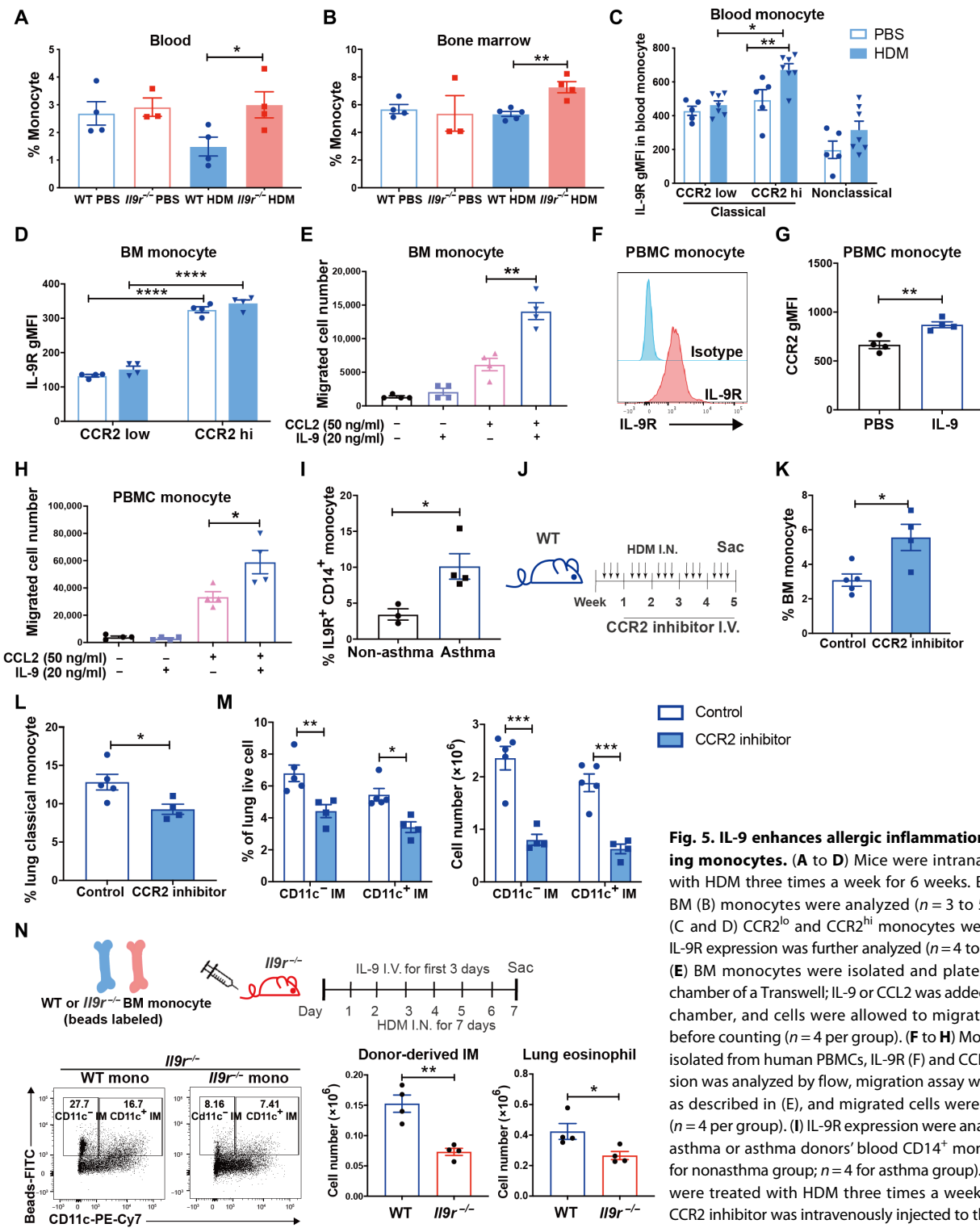


**Fig. 5. IL-9 enhances allergic inflammation via recruiting monocytes.** (A to D) Mice were intranasally treated with HDM three times a week for 6 weeks. Blood (A) and BM (B) monocytes were analyzed ( $n = 3$  to 5 per group). (C and D) CCR2<sup>lo</sup> and CCR2<sup>hi</sup> monocytes were gated and IL-9R expression was further analyzed ( $n = 4$  to 7 per group). (E) BM monocytes were isolated and plated on the top chamber of a Transwell; IL-9 or CCL2 was added to the lower chamber, and cells were allowed to migrate for 3 hours before counting ( $n = 4$  per group). (F to H) Monocytes were isolated from human PBMCs, IL-9R (F) and CCR2 (G) expression was analyzed by flow, migration assay was performed as described in (E), and migrated cells were analyzed (H) ( $n = 4$  per group). (I) IL-9R expression were analyzed in non-asthma or asthma donors' blood CD14<sup>+</sup> monocytes ( $n = 3$  for non-asthma group;  $n = 4$  for asthma group). (J to M) Mice were treated with HDM three times a week for 5 weeks. CCR2 inhibitor was intravenously injected to the mice twice a week for 4 weeks (J). BM monocytes (K), lung monocytes (L), and lung macrophages (M) were analyzed by flow cytometry ( $n = 5$  for the control group;  $n = 4$  for the CCR2 inhibitor group). (N) Fluorescent bead-labeled monocytes were transferred to II9r<sup>-/-</sup> mice, recipient mice were treated with IL-9 and HDM, lung macrophages and eosinophils were analyzed on day 7, and dot plots were gated on MerTK<sup>+</sup> CD64<sup>+</sup> Siglec<sup>-</sup> live cells ( $n = 4$  per group). Data are presented as means  $\pm$  SEM from two independent experiments. Unpaired two-tailed Student's *t* test was used for comparison to generate *P* values in (A), (B), (E), (G) to (I), (K), (L), and (N). Two-way ANOVA with Sidak's multiple comparisons was used to generate *P* values in (C), (D), and (M). \**P* < 0.05, \*\**P* < 0.01, \*\*\**P* < 0.001, and \*\*\*\**P* < 0.0001. See also fig. S5.

(L), and lung macrophages (M) were analyzed by flow cytometry ( $n = 5$  for the control group;  $n = 4$  for the CCR2 inhibitor group). (N) Fluorescent bead-labeled monocytes were transferred to II9r<sup>-/-</sup> mice, recipient mice were treated with IL-9 and HDM, lung macrophages and eosinophils were analyzed on day 7, and dot plots were gated on MerTK<sup>+</sup> CD64<sup>+</sup> Siglec<sup>-</sup> live cells ( $n = 4$  per group). Data are presented as means  $\pm$  SEM from two independent experiments. Unpaired two-tailed Student's *t* test was used for comparison to generate *P* values in (A), (B), (E), (G) to (I), (K), (L), and (N). Two-way ANOVA with Sidak's multiple comparisons was used to generate *P* values in (C), (D), and (M). \**P* < 0.05, \*\**P* < 0.01, \*\*\**P* < 0.001, and \*\*\*\**P* < 0.0001. See also fig. S5.

7 days to establish an environment for monocytes to differentiate into IMs (fig. S5F). Mice that received WT monocytes showed slightly increased donor monocytes and CD11c<sup>-</sup> IMs in the lung and significantly more CD11c<sup>+</sup> IMs than mice that received *Il9r*<sup>-/-</sup> monocytes (fig. S5, G and H). The number of AMs was not altered by the donor cells (fig. S5I). In addition, the WT but not the *Il9r*<sup>-/-</sup> monocyte recipients showed strongly elevated BALF total cell numbers, lung eosinophils, and lung inflammation (fig. S5, J to L). To assess the effect of IL-9 signaling on monocytes, fluorescent bead-labeled monocytes were transferred into *Il9r*<sup>-/-</sup> mice (Fig. 5N) (32). Flow cytometric analysis of bead-labeled monocytes showed that IL-9 signaling promotes monocytes to become lung IMs (Fig. 5N). Together, these results demonstrated that, mechanistically, IL-9 inhibited the self-renewal capacity of AMs and promoted monocyte recruitment to the lung for subsequent development into IMs. Moreover, IL-9 signaling induces the proallergic function of monocytes and IMs.

### IL-9 affects lung macrophage function by regulating Arg1 expression

Because IL-9 signaling is required for the proallergic effect of lung macrophages, we next wanted to define the underlying mechanism of IL-9-mediated lung macrophage function. We found that *Arg1* was one of the most differentially expressed genes from our CITE-seq data (Fig. 6A) and *Arg1* has been shown to be a key factor related to the pathogenesis of asthma (33). Thus, we hypothesized that *Arg1* might be a potential effector in the IL-9/macrophage axis. Consistent with our CITE-seq data, *Arg1* protein expression was substantially reduced in lung IM populations in *Il9r*<sup>-/-</sup> mice with allergic inflammation (Fig. 6B). IMs were the predominant *Arg1*<sup>+</sup> macrophages in this model (fig. S6A). In the mixed BM chimeric mice described in fig. S2D, the increased proportion of *Arg1*<sup>+</sup> IMs, but not AMs, from WT donors further confirms that IL-9 signaling regulates *Arg1* expression (Fig. 6C and fig. S6B). Because *Arg1* is also a marker for immunosuppressive macrophages and to confirm that differential expression is related to functional differences, arginase activity was measured in total lung macrophages and serum from HDM-treated mice (Fig. 6, D and E). In accordance with the diminished expression of *Arg1*, *Il9r*<sup>-/-</sup> mice also showed significantly lower arginase activity than WT mice (Fig. 6, D and E). Moreover, IL-9 promoted *Arg1* expression from IMs both in vivo and after ex vivo stimulation (Fig. 6, F and G). Loss of IL-9R did not affect *Arg1* production of IMs in response to ex vivo stimulation of IL-4 and IL-13 (fig. S6C). ILC2s have also been shown to be an important *Arg1* producer (34), and although ILC2s did expand early during the chronic challenge (fig. S6D), *Arg1* expression from ILC2s in *Il9r*<sup>-/-</sup> mice was comparable with WT mice (fig. S6E). Together, these data suggest that *Arg1* is a downstream target of IL-9 signaling in lung macrophages.

To test whether *Arg1*<sup>+</sup> macrophages contribute to IL-9-mediated allergic responses, *Arg1*-expressing or nonexpressing macrophages were sorted from *Arg1* yellow fluorescent protein (YFP) reporter (YARG) mice that were subjected to HDM challenge and subsequently transferred into *Il9r*<sup>-/-</sup> mice (Fig. 6H). YFP<sup>+</sup> macrophages migrated to the lung (Fig. 6I) and restored the *Arg1*<sup>+</sup> macrophage population in the lung of *Il9r*<sup>-/-</sup> mice (Fig. 6J). YFP<sup>+</sup> (*Arg1*<sup>+</sup>) macrophages successfully rescued allergic lung inflammation in *Il9r*<sup>-/-</sup> mice, whereas YFP<sup>-</sup> macrophages did not (Fig. 6, K to M, S6F).

To directly test the requirement for *Arg1* in allergic lung inflammation, *Arg1*<sup>fl/fl</sup>*LysM-Cre*<sup>+</sup> or littermate control mice were

challenged with HDM; *Arg1*<sup>fl/fl</sup>*LysM-Cre*<sup>+</sup> mice showed decreased *Arg1* expression in IMs and lower serum arginase activity (Fig. 7A and fig. S6G). Lung macrophages were the major *Arg1* producers in vivo (fig. S6H). Mice lacking *Arg1* expression in myeloid cells showed substantially decreased allergic inflammation, indicated by decreased BALF total numbers, BALF eosinophils, lung eosinophils, and MLN cell numbers (Fig. 7, B to E). Consistent with the decreased *Ccl5* expression from *Il9r*<sup>-/-</sup> IMs in our CITE-seq data (Fig. 7F), *Arg1*-deficient IMs also demonstrated lower *CCL5* expression than control IMs (Fig. 7G), which is also consistent with the lower level of serum *CCL5* in both *Arg1*<sup>fl/fl</sup>*LysM-Cre*<sup>+</sup> and *Il9r*<sup>-/-</sup> mice (Fig. 7, H and I). In response to IL-9 stimulation in vitro, *Arg1*<sup>+</sup> macrophages secreted more *CCL5* than *Arg1*<sup>-</sup> macrophages (Fig. 7J). IL-9 also increased *CCL5* expression from IMs in vivo (Fig. 7K). Furthermore, IL-9 expanded the *Arg1*<sup>+</sup> *CCL5*<sup>+</sup> IM population in naïve mice, and *CCL5* is exclusively expressed in *Arg1*<sup>+</sup> IMs (Fig. 7L). Moreover, in a uniform inflammatory environment, *Arg1*<sup>+</sup> IMs from HDM-treated mice expressed more *CCL5* than *Arg1*<sup>-</sup> IMs (Fig. 7M). These results suggest that IL-9 regulation of allergic airway inflammation requires *Arg1* expression in lung macrophages, and *Arg1*<sup>+</sup> IMs secrete more *CCL5* to induce eosinophil-mediated allergic inflammation.

Consistent with the results from murine cells, IL-9 promotes *CCL5* expression from human BM-derived macrophages (Fig. 7N). To further detect whether this paradigm is observed in patient samples, we analyzed IL-9 concentration and arginase activity from a well-defined population of atopic children (29, 30), and IL-9 produced from infant PBMCs was inversely correlated with parameters of lung function (35). Atopic children with asthma diagnosis at age of 5 years showed increased IL-9 production from anti-CD3-stimulated PBMCs that was inversely correlated with lung function and associated with increased serum arginase activity compared with children that are atopic but did not have physician-diagnosed asthma (Fig. 7, P and Q). Compared with nonasthmatic patients, asthmatic patients also showed increased *CCL5* expression (Fig. 7R). IL-9 production is positively correlated to serum *CCL5* level (Fig. 7S). Collectively, these data suggest that IL-9 regulates allergic airway inflammation by increasing the expression of *Arg1* and *CCL5* in lung macrophages.

### DISCUSSION

Lung macrophages play an important role in maintaining immune homeostasis and fine-tuning immune responses. During an immune response, de novo monocytes migrate to inflammatory sites and develop into macrophages. Monocyte-derived macrophages had been regarded as a uniform IM population (1, 36). Recently, emerging studies showed that IMs are actually heterogeneous and can be distinguished into Lyvel<sup>lo</sup> MHCII<sup>hi</sup> CX3CR1<sup>hi</sup> and Lyvel<sup>hi</sup> MHCII<sup>lo</sup> CX3CR1<sup>lo</sup> populations (4). Additional studies defined IM populations using expression of CD206, CD11c, and major histocompatibility complex II (MHCII) (3, 4, 37). However, these studies focused on the classification of IMs in a steady state, and only some of them showed functional differences among the subsets in type 1 immune response (5, 38). Focusing on the heterogeneity and function of lung macrophages in allergic disease, this report demonstrates how lung macrophages contribute to IL-9-mediated allergic inflammation. Our results demonstrate that macrophage populations are among the cells that express the most IL-9R in the allergic lung. IMs are

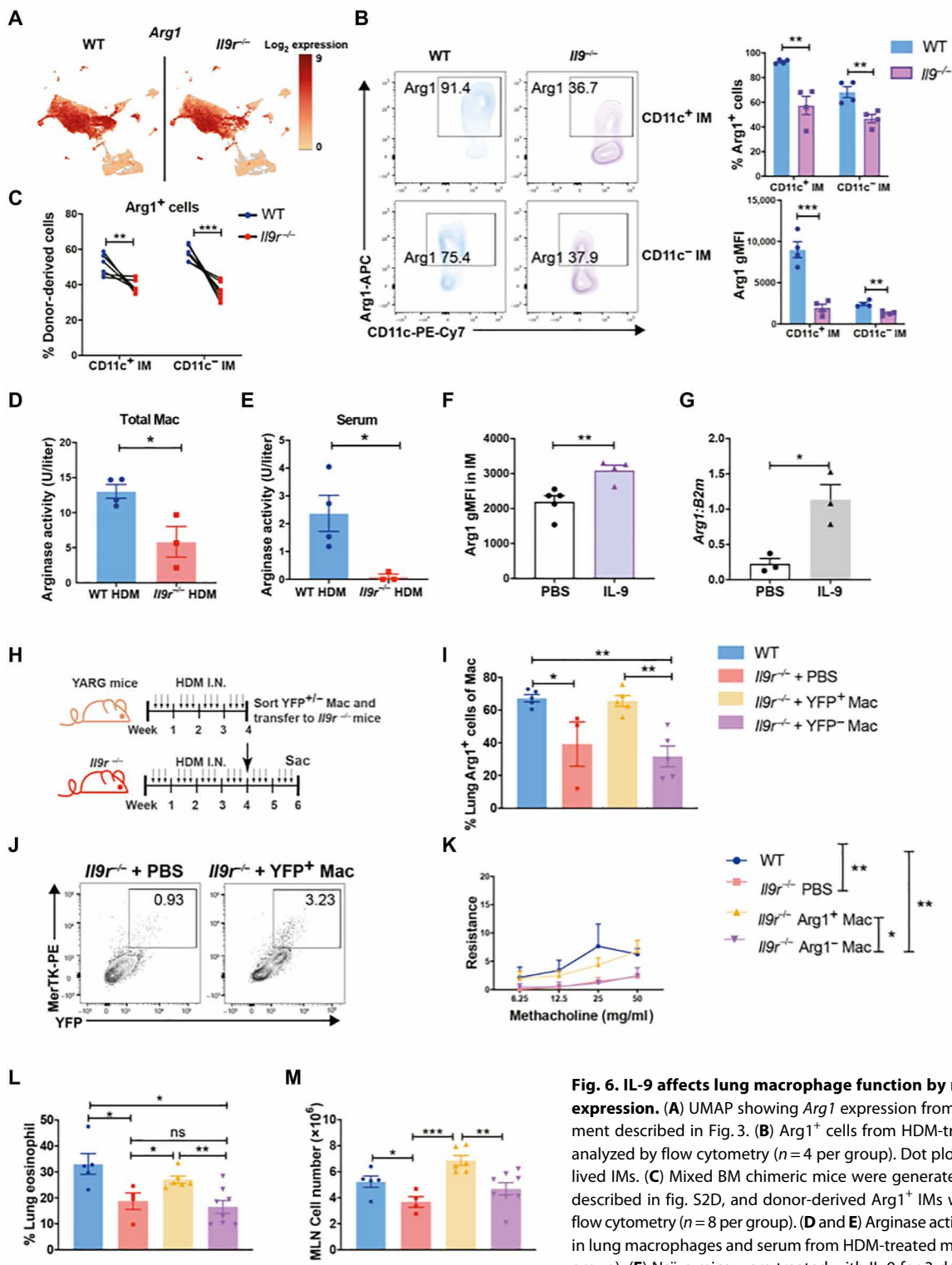


**Fig. 6. IL-9 affects lung macrophage function by regulating Arg1 expression.** (A) UMAP showing *Arg1* expression from CITE-seq experiment described in Fig. 3. (B) *Arg1*<sup>+</sup> cells from HDM-treated mice were analyzed by flow cytometry ( $n = 4$  per group). Dot plots were gated on live IMs. (C) Mixed BM chimeric mice were generated and treated as described in fig. S2D, and donor-derived *Arg1*<sup>+</sup> IMs were analyzed by flow cytometry ( $n = 8$  per group). (D and E) Arginase activity was analyzed in lung macrophages and serum from HDM-treated mice ( $n = 3$  to 4 per group). (F) Naïve mice were treated with IL-9 for 3 days; *Arg1* production from IMs were analyzed ( $n = 5$  for the PBS group;  $n = 4$  for the IL-9-treated group). (G) IMs were sorted from WT HDM-treated mice and stimulated with IL-9 for 24 hours; *Arg1* mRNA expression was analyzed ( $n = 3$ ). (H to M) YARG and *Il9<sup>-/-</sup>* mice were treated with HDM three times a week for 4 weeks. YFP<sup>+/−</sup> macrophage (Mac) populations were sorted from YARG mice 1 day after the last HDM treatment and intranasally transferred to *Il9<sup>-/-</sup>* mice, followed by HDM challenge every other day for another 2 weeks (H). Lung *Arg1*<sup>+</sup> macrophages (I) and YFP<sup>+</sup> macrophages (J) were analyzed by flow cytometry. (K) Airway resistance was measured in response to methacholine challenge 1 day after the last HDM treatment at the end of week 6. Statistical differences are indicated between groups in the panel key for clarity. (L) Lung eosinophils were analyzed by flow. (M) MLN cell number was analyzed ( $n = 3$  to 8 per group). Data are presented as means  $\pm$  SEM from two independent experiments. Paired two-tailed *t* tests were used to generate *P* values in (B) and (C). Unpaired two-tailed Student's *t* test was used for comparison in (D) to (G), (L), and (M). One-way ANOVA with Tukey's multiple comparisons was used to generate *P* values in (I). Two-way ANOVA with Tukey's multiple comparisons was used to generate *P* values in (K) to compare group effect using the mean of every group. \**P* < 0.05, \*\**P* < 0.01, and \*\*\**P* < 0.001. See also fig. S6.

tion from IMs were analyzed ( $n = 5$  for the PBS group;  $n = 4$  for the IL-9-treated group). (G) IMs were sorted from WT HDM-treated mice and stimulated with IL-9 for 24 hours; *Arg1* mRNA expression was analyzed ( $n = 3$ ). (H to M) YARG and *Il9<sup>-/-</sup>* mice were treated with HDM three times a week for 4 weeks. YFP<sup>+/−</sup> macrophage (Mac) populations were sorted from YARG mice 1 day after the last HDM treatment and intranasally transferred to *Il9<sup>-/-</sup>* mice, followed by HDM challenge every other day for another 2 weeks (H). Lung *Arg1*<sup>+</sup> macrophages (I) and YFP<sup>+</sup> macrophages (J) were analyzed by flow cytometry. (K) Airway resistance was measured in response to methacholine challenge 1 day after the last HDM treatment at the end of week 6. Statistical differences are indicated between groups in the panel key for clarity. (L) Lung eosinophils were analyzed by flow. (M) MLN cell number was analyzed ( $n = 3$  to 8 per group). Data are presented as means  $\pm$  SEM from two independent experiments. Paired two-tailed *t* tests were used to generate *P* values in (B) and (C). Unpaired two-tailed Student's *t* test was used for comparison in (D) to (G), (L), and (M). One-way ANOVA with Tukey's multiple comparisons was used to generate *P* values in (I). Two-way ANOVA with Tukey's multiple comparisons was used to generate *P* values in (K) to compare group effect using the mean of every group. \**P* < 0.05, \*\**P* < 0.01, and \*\*\**P* < 0.001. See also fig. S6.

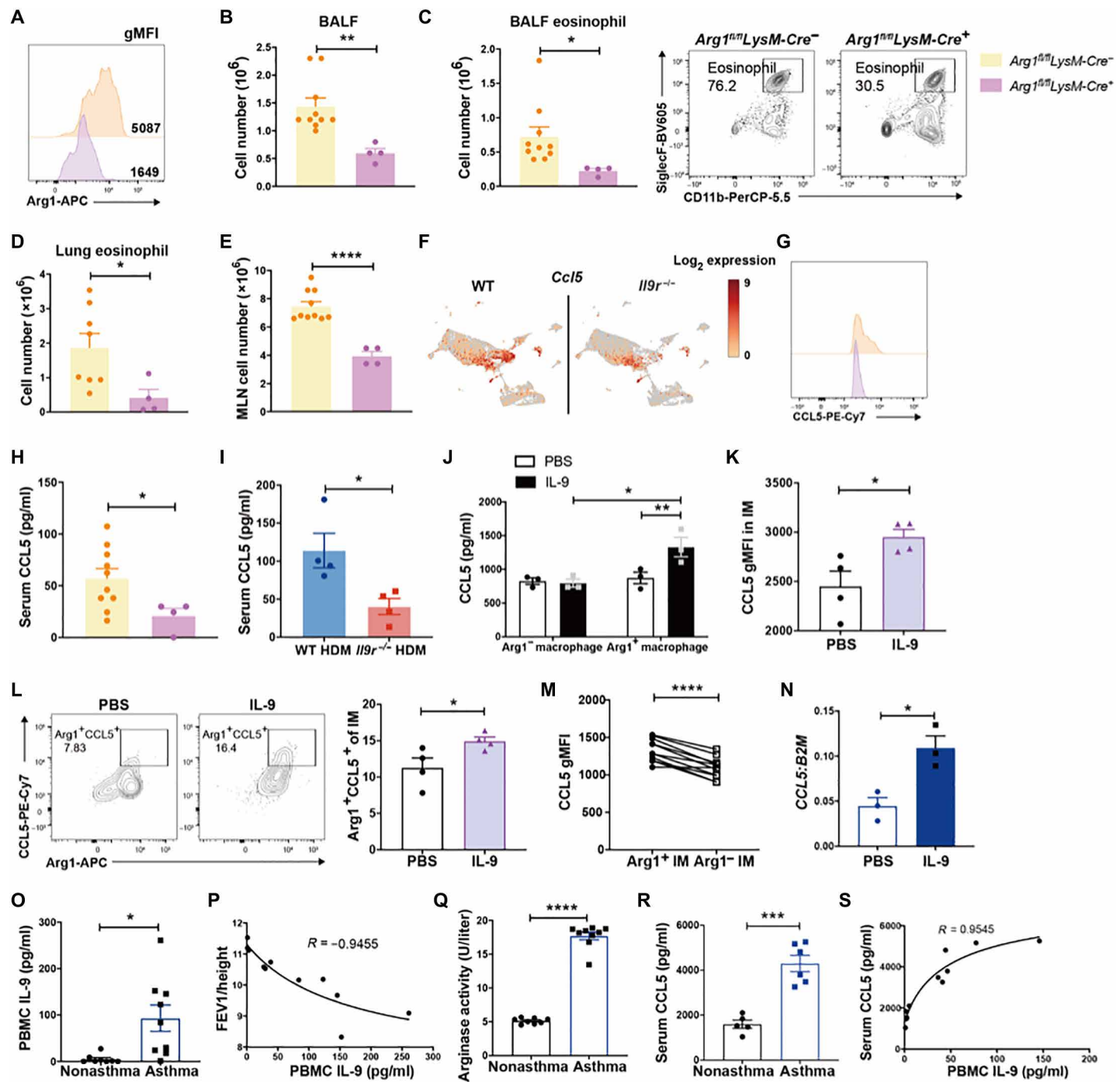


**Fig. 7. IL-9 promotes allergic inflammation by inducing CCL5 production from lung macrophages.** *Arg1<sup>f/f</sup> LysM-Cre<sup>+/−</sup>* mice were treated with HDM for 6 weeks. (A) Arg1 expression in IMs was analyzed. BALF total cell number (B), BALF eosinophils (C), lung eosinophils (D), and MLN cell number (E) were analyzed ( $n = 4$  to 10). (F) UMAP showing *Ccl5* expression from CITE-seq experiment described in Fig. 3. (G) CCL5 expression in IMs was analyzed by flow cytometry ( $n = 4$  to 10). (H and I) Serum CCL5 level was analyzed by ELISA ( $n = 4$  to 10). (J) FACS-sorted Arg1<sup>+/−</sup> macrophages were treated with IL-9 for 24 hours; CCL5 level was measured by ELISA ( $n = 3$ ). (K and L) Naïve mice were treated with IL-9 for 3 days; CCL5 and Arg1 expression from IMs were analyzed ( $n = 4$ ). (M) CCL5 expression was analyzed by gating on Arg1<sup>+/+</sup> or Arg1<sup>-/-</sup> IMs from WT HDM-treated mice ( $n = 11$ ). (N) Human monocyte were cultured under M2 macrophage condition; CCL5 mRNA expression was analyzed ( $n = 3$ ). (O) IL-9 production from PBMCs was analyzed from nonasthma donors and patients with asthma ( $n = 7$  to 9). (P) Correlation between first second of forced expiration (FEV1) corrected for height and IL-9 production from patient PBMCs. (Q and R) Arginase activity (Q) and CCL5 level (R) were analyzed from nonasthma donors and patients with asthma ( $n = 5$  to 9). (S) Correlation of PBMC IL-9 and serum CCL5 concentration ( $n = 11$ ). Data are presented as means  $\pm$  SEM from two independent experiments. Unpaired two-tailed Student's *t* test was used for comparison in (B) to (E), (H), (I), (K), (L), (N), (O), (Q), and (R). A paired two-tailed *t* test was used to generate the *P* value in (M). Two-way ANOVA with Sidak's multiple comparisons was used for comparisons in (J). Spearman correlation was performed for (P) and (S). \**P* < 0.05, \*\**P* < 0.01, \*\*\**P* < 0.001, and \*\*\*\**P* < 0.0001. See also fig. S6. BV605, Brilliant Violet 605; PerCP, peridinin-chlorophyll-protein.

capable of conferring IL-9R-dependent allergic inflammation in *Il9r<sup>-/-</sup>* mice. Critical target genes of IL-9R signaling include *Arg1* and *Ccl5*, and *Arg1* is required for macrophages to promote allergic inflammation. We also found evidence that this pathway is conserved in human asthma patient samples.

IL-9 is known to enhance type 2 immune responses in allergic diseases (6), with mast cells being direct IL-9-responsive cells in asthma (15, 18). Additional studies have implicated IL-9 in the functions of multiple cell types, including T helper 2 cells, epithelial cells, and B cells (9, 14, 16). However, knowledge about IL-9-targeted cells is still limited. In this study, we assessed IL-9R expression across various cell types to identify IL-9-responsive populations in allergic airway inflammation. Unexpectedly, lung macrophages occupied a substantial proportion of the IL-9R<sup>+</sup> cells. They also express relatively high amounts of IL-9R compared with other cell types, such as eosinophils and neutrophils. Now, only a few studies have focused on the direct impact of IL-9 on macrophages, including identifying microglia as a downstream target of IL-9 in multiple sclerosis. Moreover, IL-9R expression has been detected in human blood monocytes and AMs (20, 21, 39). Overall, IL-9 regulation of IMs in diseases states is poorly understood. Our results suggest that lung macrophages are not only an IL-9-responsive population but also a key driver of the allergic response by secreting *Arg1* and eosinophil-attracting chemokines.

A recent report showed the presence of the CD11c<sup>+</sup> IMs in ovalbumin-induced allergic inflammation (40). Here, we found that the induction of CD11c<sup>+</sup> IMs is highly dependent on IL-9 signaling. This population acts as a key component for IL-9-mediated allergic responses, demonstrated by the restoration of disease progression in adoptive transfer experiments. Although this study has advanced the understanding of the functions of lung IM in the allergic environment, further studies are required to investigate the transition from monocytes to IM populations in various microenvironments, their biological functions in specific inflammatory responses, and their transcriptional programs.

*Arg1* is one of the most important enzymes that regulates macrophage functions (41) and is a marker of macrophage alternative activation. Demonstration of *Arg1* function in asthma models has been controversial and may vary with the model or genetic background of the mice (42–50). In particular, Barron *et al.* (51) used *Arg1* conditional mutant mice on a BALB/c background and with Cre expression that deleted in all hematopoietic cells, demonstrating a limited role for *Arg1* in lung inflammation. Our studies deleted *Arg1* more specifically in the myeloid compartment and were on a C57BL/6 background. It is possible that differences are observed because of compensation resulting from deletion in distinct populations between the models or from differences in protocols. It is also possible that in a genetic environment that is highly skewed toward type 2 inflammation as in the BALB/c mice, *Arg1* is dispensable. In our studies, however, *Arg1* in macrophages is clearly required. In immune models where *Arg1* function has been demonstrated, it appears to suppress inflammation potentially by depleting Arg in the environment (52, 53). This suppressive function is not consistent with the proallergic function observed in our preliminary data and other studies, as well as patient samples where increased *Arg1* expression and arginase activity are associated with progressive asthma development (33, 42–44). Together, these observations suggest that the function of *Arg1* in the lung may be dependent on the inflammatory milieu and the genetic environment.

The stimuli for *Arg1* expression in lung macrophages during disease is still not clear. Previous studies have shown that IL-4 and IL-13 can induce *Arg1* expression and promote an immunosuppressive macrophage phenotype (41). Here, we found that IL-9 induced *Arg1* expression in lung macrophages in both naïve and HDM-treated mice. Using mixed BM chimeric mice, we found that IL-9 signaling in IMs is intrinsically required for *Arg1* expression. *Il9r<sup>-/-</sup>* IMs express IL-4R and responded to IL-4 or IL-13 to induce *Arg1*, indicating the requirement for IL-9 even in the presence of normal IL-4/IL-4R-induced *Arg1* expression. Collectively, these results suggest that *Arg1* is an important effector for IL-9-mediated macrophage function. Further investigations on how IL-9 promotes *Arg1* expression in lung macrophages and whether this regulation is conserved in other diseases are required.

ILC2s have been shown to be important IL-9 producers and responders (11, 54) and are particularly important in acute allergic inflammation. ILC2s have also been shown to produce *Arg1* in type 2 inflammation (34), but *Arg1* expression in ILC2s in the chronic allergic airway inflammation model was not impaired in the absence of IL-9 signaling. Moreover, the studies using clodronate depletion, macrophage adoptive transfer, and myeloid cell deletion of *Arg1* argue against ILC2s as responders to IL-9 or as sources of *Arg1*. Thus, although ILC2s are important for the development of allergic inflammation in some contexts, there is no evidence that they contribute to the IL-9/macrophage/*Arg1* axis described here that is critical for chronic airway inflammation.

Our CITE-seq analysis showed that expression of multiple chemokines was down-regulated in IL-9R-deficient macrophages. Among them, we found that IL-9 signaling promotes *CCL5* expression in both mouse and human macrophages. In asthmatic patients, *CCL5* promotes disease progression by recruiting eosinophils to the airway, a function that has been recapitulated in mouse models as well (55, 56). Our results suggest that IL-9 stimulates *Arg1<sup>+</sup>* IMs to secrete *CCL5*. This is a potential explanation for why *Arg1<sup>+</sup>* macrophages rescue the allergic response in IL-9R-deficient mice and why the loss of IL-9 signaling hinders the proallergic function of lung macrophages. Thus, blocking IL-9 signaling in lung macrophages could be a feasible therapeutic strategy for asthma and potentially other pulmonary inflammatory diseases.

## MATERIALS AND METHODS

### Study design

The aim of this study was to characterize the IL-9-responsive cells in allergic inflammation and to uncover the mechanisms of the development of IL-9-mediated allergic diseases. Using flow cytometry, we demonstrated that macrophage populations had high expression of IL-9R and that populations were substantially altered in the absence of IL-9 signaling. By performing CITE-seq analysis, liposome clodronate-mediated macrophage depletion assays, adoptive transfer experiments, and morphology analysis, we demonstrated that IL-9 signaling promotes monocyte migration and differentiation into CD11c<sup>+</sup> IMs and CD11c<sup>-</sup> IMs. We used adoptive transfer experiments and IL-9/IL-9R-deficient mice to show that IMs are required for IL-9-mediated allergic inflammation. Moreover, by using *Arg1* reporter mice and *Arg1* conditional knockout (KO) mice, we found that *Arg1* was required for IL-9-dependent proallergic activity in macrophages. Last, we confirmed that the IL-9/lung macrophage axis is conserved in human patients with asthma using biobanked

patient samples. The number of mice used in the studies is included in the figure legends.

### Mice

All mice were on C57BL/6 background. WT mice (C57BL/6, 002014), Boy/J mice (C57BL/6, 002014), *Il4*<sup>-/-</sup> mice, YARG mice (C57BL/6, 015857) (57), *Arg1*<sup>fl/fl</sup> mice (C57BL/6, 008817), and *LysM-Cre* (C57BL/6, 004781) were purchased from the Jackson Laboratory. *Il9*<sup>-/-</sup> mice (C57BL/6) were gift from J.-C.R. (58). *Il9*<sup>-/-</sup> mice (C57BL/6) were provided by A. McKenzie and coworkers (59), A. Kirsch, and S.P. Infer mice were provided by P.L.-L. and R.A.F. Both female and male mice were used between the ages of 8 to 16 weeks. All the mice were maintained in specific pathogen-free animal facilities (ambient temperature of 21° to 22°C, humidity of 50%, light/dark cycle of 12 hours/12 hours). All experiments were performed with the approval of the Indiana University Institutional Animal Care and Use Committee.

### Patient samples

Patients were recruited in infancy from pediatric allergy and dermatology clinics associated with IU (Indiana University) Health and Riley Children's Hospital based on a diagnosis of dermatitis. Participants were excluded for a history of prior wheezing, lower respiratory tract illness, treatment with asthma medications, or congenital heart disease. The majority of the population (85%) had a family history of asthma or allergy, which was used as the criteria for high risk. Samples in this study were a subset of patients that were physician-diagnosed with or without asthma at age of 5 based on parameters including persistent wheezing, the requirement for asthma-controlling medications, respiratory function, and response to methacholine challenge (60). The primary outcome of this cohort was to analyze airway function in a high-risk population of infants (30, 31, 35). All studies with human participants and samples were performed with approval from the Indiana University Institutional Review Board and required informed consent from a parent or guardian. All participants were evaluated at the James Whitcomb Riley Hospital for Children, Indianapolis, Indiana. Characteristics of the subset of patients selected for the presence or absence of physician-diagnosed asthma for this study are listed in table S2. Patient sample collection and analysis were approved by the Institutional Review Board of Indiana University and required parental consent for samples from infants.

### Induction of allergic airway inflammation

Mice were challenged intranasally with HDM (Greer Laboratories) or ASP (Greer Laboratories) extract three times a week for 6 weeks. HDM or ASP (25 µg) extract was diluted with PBS (25 µl) and administered into the nose. Mice were euthanized 1 day after final intranasal challenge. Mice were euthanized and lungs were lavaged two times with cold PBS. BALF was collected, and cells were centrifuged at 1500g for 5 min at 4°C for further surface staining. The supernatant was saved at -80°C for enzyme-linked immunosorbent assay (ELISA) analysis. The rest of the lung tissue was digested in collagenase A (0.5 mg/ml; Roche) medium for 1 hour at 37°C with rotation. After digestion, the lungs were filtered through mesh, and red blood cells were lysed with ACK lysis buffer for 3 min (Lonza). One million cells were kept for RNA analysis. Cells were washed with fluorescence-activated cell sorting (FACS) buffer and stained for granulocytes, mast cells, and lymphocytes. Eosinophils were identified as live Ly6G<sup>-</sup> SiglecF<sup>+</sup> CD11c<sup>-</sup> CD11b<sup>+</sup> cells. Neutrophils

were identified as live Ly6G<sup>+</sup> CD11b<sup>+</sup> cells. Mast cells were identified as CD49b<sup>-</sup> FcεR1<sup>+</sup> c-Kit<sup>+</sup> cells. Monocytes were identified as live Ly6c<sup>+</sup> CD11b<sup>+</sup> cells. DCs were identified as live MHCII<sup>+</sup> CD11b<sup>+</sup> or MHCII<sup>+</sup> CD103<sup>+</sup> cells. Total macrophages were identified as live CD64<sup>+</sup> MerTK<sup>+</sup> cells. AMs, CD11c<sup>-</sup> IMs, and CD11c<sup>+</sup> IMs were distinguished by the expression of SiglecF and CD11c. Blood was collected by cardiac puncture. A portion of the blood was kept for FACS analysis; red blood cells were lysed with ACK lysis buffer for 3 min (Lonza). The remaining blood samples were kept for serum. The serum was taken after centrifugation at 14,000 rpm for 10 min at 4°C. For some of the experiments, the CCR2 inhibitor (2 mg/kg; R&D Systems, RS 504393) was intravenously injected to the mice for 3 weeks. Anti-IL-9 (Bio X Cell, 9C1), anti-IL-13(R&D Systems, MAB413) antibodies, and their isotype IgG antibodies were intravenously injected to the mice every other day for 2 weeks.

### Airway resistance

For airway resistance, mice were subjected to increasing doses of methacholine, and airway resistance was measured using a ventilator (Elan Series Mouse RC Site, Buxco Electronics) and BioSystem XA software (Buxco Electronics).

### Macrophage depletion

Mice were challenged with 150 µl of clodronate intranasally or 200 µl of clodronate intravenously every other day for 2 weeks. Mice were euthanized 1 day after the final challenge. The subsequent procedures for sample harvesting are the same as for the HDM extract- or ASP extract-induced allergic airway inflammation experiment.

### Cell migration assay

Monocyte migration assay was performed by using CytoSelect 24-well cell migration assay kit (Cell Biolabs Inc.). Mouse BM-derived monocytes were isolated by magnetic selection according to the company protocol (Miltenyi Biotec, monocyte isolation kit, 130-100-629). Monocytes [0.5 × 10<sup>6</sup> in 100 µl of serum-free Dulbecco's modified Eagle's medium (DMEM) containing 1% bovine serum albumin (BSA)] were added to the upper chamber of the insert. The lower chamber contained 400 µl of complete DMEM with or without cytokine and chemokine as indicated. The plates were incubated at 37°C in 5% CO<sub>2</sub> incubator for 3 hours, and cells that migrated into the lower chamber were counted.

### IL-9 injection model

Mice were treated with 4 µg of IL-9 (BioLegend, 556004) intravenously or intraperitoneally for 3 days. Mice were euthanized 1 day after the final intranasal challenge. The subsequent procedures for sample harvesting are the same as for the HDM extract- or ASP extract-induced allergic airway inflammation experiment.

### Arginase activity assay

For measurements of arginase activity, we harvested ~10<sup>6</sup> cells per sample and centrifuged at 1000g at 4°C for 10 min. Cell pellets were lysed for 10 min in 100 µl of 10 mM tris-HCl (pH 7.4) containing 1 µM pepstatin A, 1 µM leupeptin, and 0.4% (w/v) Triton X-100. The cell lysate was centrifuged at 14,000g at 4°C for 10 min, and used supernatant was assessed for arginase activity using the QuantiChrom Arginase Assay Kit (BioAssay Systems) according to the manufacturer's directions.

### Mixed BM chimera

The F<sub>1</sub> generation of CD45.1 × CD45.2 mice was irradiated at 10 Gy. One day after the irradiation, 8 million BM cells (4 million from Boy/J mice and 4 million from *Il9r*<sup>-/-</sup> mice) were injected to the recipient mice. Mice were used 12 weeks after donor cell injection.

### Macrophage transfer

Lung macrophage populations were sorted from HDM-treated mice. Cells were transferred into *Il9r*<sup>-/-</sup> mice (0.3 million from Boy/J mice and 0.15 million from YARG mice). Recipient mice were harvested as indicated in the figures.

### Mouse BM-derived macrophage cell polarization

BM cells were isolated, and red blood cells were lysed by using ACK buffer. Cells (0.5 million/ml) were cultured with complement DMEM containing 20% L929 supernatant (Cell Biologics, 3368) for 7 days. Interferon-γ (IFN-γ) (50 ng/ml; PeproTech) for M1 macrophages or IL-4 (20 ng/ml; PeproTech) for M2 macrophages were added on day 7 for 24 hours.

### Human macrophage polarization

Deidentified buffy coat blood packs from healthy donors were purchased from Indiana Blood Center. PBMCs were isolated by density gradient centrifugation using Ficoll-Paque (GE Healthcare). Buffy coat cells (10 ml) were diluted with 10 ml of Dulbecco's PBS and gently added to 15 ml of Ficoll-Paque. After spinning down at 400g for 30 min at room temperature (RT) without brake, the upper layer was removed. The mononuclear cell layer was collected and transferred to a new conical tube and filled with MACS buffer up to 50 ml. After mixing, cells were centrifuged at 300g for 10 min, repeating this washing step three times. Human naïve CD14<sup>+</sup> monocytes were isolated from the PBMCs using magnetic separation (Miltenyi Biotec). Cells were cultured in the presence of granulocyte-macrophage colony-stimulating factor (GM-CSF) (50 ng/ml; PeproTech) or M-CSF (50 ng/ml; PeproTech) for differentiating to M1 or M2 macrophages for 7 days. IFN-γ (20 ng/ml; PeproTech) or IL-4 (20 ng/ml; PeproTech) was added for 48 hours. Cells were harvested for further analysis.

### Cell hashing and CITE-seq

Total lung macrophages and blood monocytes were sorted from HDM-treated mice. Ten mice were pooled for each group before sorting. Sorted cells were labeled with cell hashing antibodies and CITE-seq antibodies according to the CITE-seq and Cell Hashing Protocol version 2019-02-13 ([cite-seq.com/protocols](http://cite-seq.com/protocols)) (61, 62). Briefly, blood monocytes were stained with TotalSeq-A0302 anti-mouse Hashtag 1 antibody (BioLegend) for 30 min at 4°C. Lung macrophages were stained with CD11c-TotalSeq A (BioLegend), SiglecF biotin antibody, and TotalSeq-A0301 anti-mouse Hashtag 1 antibody (BioLegend) for 30 min at 4°C. After washing three times, lung macrophages were stained with a secondary anti-biotin-TotalSeq A antibody (BioLegend) for 30 min. The final single-cell suspension was washed three times with 0.1% BSA in PBS. Each clean single-cell suspension was counted with a hemocytometer under a microscope for cell number and cell viability. Labeled lung macrophages and blood monocytes were pooled at the ratio of 3:1. Twenty thousand targeted cell recovery per sample pool were super loaded to a single-cell master mix with lysis buffer and reverse transcription

reagents, following the Chromium Single Cell 3' Reagent Kits V3 User Guide, CG000183 Rev. A (10X Genomics Inc.). Along with the single-cell gel beads and partitioning oil, the single-cell master mixture containing the cells was dispensed onto a single-cell chip B in separate wells, and the chip loaded to the Chromium Controller for Gel Bead-In EMulsions (GEM) generation and barcoding, followed by reverse transcription. During cDNA amplification, HTO and ADT polymerase chain reaction (PCR) additive oligonucleotides were spiked into the 10X cDNA amplification to increase the yield of HTO and ADT products. After cDNA amplification, each sample was separated into ADT-derived [<180 base pairs (bp)], HTO-derived (<180 bp), and mRNA-derived cDNAs (>300 bp). The mRNA-derived cDNAs were further processed with the standard 10X Genomics protocol. The ADT and HTO libraries were prepared using the Illumina TruSeq Small RNA adapter and Illumina TruSeq adapter sequences, respectively. At each step, the quality and quantity of cDNA and library were examined by Bioanalyzer and Qubit. The resulting libraries were pooled at a ratio of 5:10:85 of HTO, ADT, and mRNA in molarity and sequenced on an Illumina NovaSeq 6000. About 6000 antibody reads per cell of ADT and HTO and 40,000 to 50,000 reads per cell of mRNA were generated, with 28 bp of read 1 of cell barcode and unique molecular identifier (UMI) and 91 bp of read 2 of RNA or HTO/ADT.

### Analysis of cell hashing and CITE-seq

CellRanger 3.1.0 (<http://support.10xgenomics.com/>) was used to process the raw sequence data generated. Briefly, CellRanger used bcl2fastq (<https://support.illumina.com/>) to demultiplex raw base sequence calls generated from the sequencer into sample-specific FASTQ files. The FASTQ files were then processed with the CellRanger count pipeline with feature barcode analysis to generate matrices of gene expression counts alongside HTO and ADT quantifications for each cell barcode. Mouse reference genome GRCm38 was used in the sequence data alignment and counting processes. The filtered feature-cell barcode matrices generated from CellRanger were used for further analysis with the R package Seurat (Seurat 3.1.1) (63, 64) with RStudio version 1.2.5001 and R version 3.5.1. To identify tissue origin of cells in the WT and KO samples, the HTO counts were normalized using centered log-ratio transformation, and cells were demultiplexed with the HTODemux function. Doublets and negative cells identified from demultiplexing were removed from further analysis. Cells with low number of detected genes/UMIs and high mitochondrial gene content were excluded as well. For gene expression data analysis, gene expression levels for each cell were log-normalized with the NormalizeData function in Seurat. Highly variable genes were subsequently identified with FindVariableFeatures using the "vst" approach. To integrate the single-cell data of the WT and *Il9r*<sup>-/-</sup> samples, functions FindIntegrationAnchors and IntegrateData from Seurat were applied. The integrated data were scaled and principal components analysis was performed. Clusters were identified with the Seurat functions FindNeighbors and FindClusters. The FindConservedMarkers function was subsequently used to identify cell cluster-specific marker genes. Cell cluster identities were manually defined with the cluster-specific marker genes or known marker genes and small populations that stained with ADT-SiglecF antibodies but were negative for transcripts encoding SiglecF or were obviously not macrophage/monocyte populations were excluded from analyses as indicated. The cell clusters were visualized using the *t*-distributed stochastic

neighbor embedding plots and UMAP plots. Analysis of the cell surface epitope expression ADT data was performed following the standard Seurat workflow of multimodal data ([https://satijalab.org/seurat/v3.1/multimodal\\_vignette.html](https://satijalab.org/seurat/v3.1/multimodal_vignette.html)).

### Real-time quantitative PCR analysis

RNA was extracted using TRIzol reagent (Thermo Fisher Scientific) or the RNeasy Plus Micro Kit (QIAGEN). cDNA synthesis was performed according to the manufacturer's instructions (qScript cDNA Synthesis Kits, Quantabio). TaqMan real-time PCR assay (Thermo Fisher Scientific) was used for detecting gene expression (table S3). The relative mRNA expression was normalized to housekeeping gene expression ( $\beta_2$ -microglobulin).

### Flow cytometry

Single-cell suspensions were stained with a fixable viability dye (eBioscience) and antibodies for surface markers for 30 min at 4°C, before fixation with 4% formaldehyde for 10 min in the dark at RT. After fixation, cells were permeabilized with permeabilization buffer (eBioscience) for 30 min at 4°C and stained for cytokines for another 30 min at 4°C. For transcription factor staining, after surface staining, cells were fixed with the Fixation and Permeabilization Buffer (eBioscience) for 2 hours or overnight at 4°C, and then permeabilized with permeabilization buffer (eBioscience). After intracellular staining, cells were washed with FACS buffer and analyzed by LSR4 or Fortessa (BD Biosciences) and analyzed with FlowJo 10.7.1 software (Tree Star).

### Cell sorting

Mouse macrophage were stained with anti-CD64, anti-Mertk, anti-CD11c, and anti-SiglecF antibody and viability dye and further sorted with FACSAria or SORPArria (BD Biosciences) by gating on live cells. Human patient samples were stained with viability dye, anti-hCD14 antibody, followed by FACS. Sorted cells were used for further experiments. Details of antibodies are listed in table S1.

### Enzyme-linked immunosorbent assay

IL-9 (BioLegend), CCL5 (Invitrogen), and HDM-specific IgE ELISA were performed according to the manufacturer's instruction. Briefly, 96-well plates were coated with coating antibody overnight at 4°C. After washing three times with the wash buffer, 300  $\mu$ l of ELISA buffer was added to the plate and incubate at RT for 2 hours. After washing three times with washing buffer, 100- $\mu$ l samples were added to the plate and incubated at RT for 2 hours. After washing three times, 100  $\mu$ l of diluted detection antibody was added to the plate and incubated at RT for 1 hour. After washing the plate three times, 100  $\mu$ l of diluted Avidin–horseradish peroxidase solution was added to the plate and incubated at RT for 30 min in the dark. After washing the plate three times, 100  $\mu$ l of the substrate was added to the plate. Plates were read at absorbance of 450 and 570 nm.

### Cytospin

Isolated lung macrophages were washed with cold PBS and resuspended with up to 200  $\mu$ l of PBS at a density of  $0.1 \times 10^6$  cells/ml. After the cytopsin at 600 rpm for 5 min, slides were stained with a modified Wright–Giemsa stain on a Hema-Tek 2000 slide stainer (Bayer Corp., Diagnostics Division, Leverkusen, Germany). The morphology of the isolated lung macrophages was evaluated under a microscope, and photos were taken.

### Immunofluorescence staining

Frozen tissue sections (5  $\mu$ m) were recovered at RT. Slides were washed three times with PBST and blocked with donkey serum at RT for 1 hour. After blocking, sections were incubated with anti-CD45.1 antibody at 4°C overnight. After washing three times, sections were incubated with goat anti-mouse IgG H&L (Alexa Fluor 488) at RT for 1 hour. After washing three times with PBST, nuclear were stained with 4',6-diamidino-2-phenylindole.

### Histology

Lung tissue was fixed with 4% formalin for 24 hours at RT. Tissues were embedded in paraffin, sectioned, and further stained with hematoxylin and eosin (H&E), periodic acid–Schiff (PAS), and toluidine blue staining.

### Statistics analysis

Statistical analysis was analyzed using GraphPad Prism 8.0 (GraphPad Software) and presented as means  $\pm$  SEM. Unpaired or paired Student's *t* tests and one-way or two-way analysis of variance (ANOVA) analysis were used in data analysis. A *P* < 0.05 was considered statistically significant. ns, *P* > 0.05; \**P* < 0.05; \*\**P* < 0.01; \*\*\**P* < 0.001; \*\*\*\**P* < 0.0001.

### SUPPLEMENTARY MATERIALS

[www.science.org/doi/10.1126/scimmunol.abi9768](http://www.science.org/doi/10.1126/scimmunol.abi9768)

Figs. S1 to S6

Tables S1 to S3

Data file S1

[View/request a protocol for this paper from Bio-protocol.](#)

### REFERENCES AND NOTES

1. T. Hussell, T. J. Bell, Alveolar macrophages: Plasticity in a tissue-specific context. *Nat. Rev. Immunol.* **14**, 81–93 (2014).
2. S. Epelman, K. J. Lavine, G. J. Randolph, Origin and functions of tissue macrophages. *Immunity* **41**, 21–35 (2014).
3. S. L. Gibbings, S. M. Thomas, S. M. Atif, A. L. McCubbrey, A. N. Desch, T. Danhorn, S. M. Leach, D. L. Bratton, P. M. Henson, W. J. Janssen, C. V. Jakubzik, Three unique interstitial macrophages in the murine lung at steady state. *Am. J. Respir. Cell Mol. Biol.* **57**, 66–76 (2017).
4. S. Chakarov, H. Y. Lim, L. Tan, S. Y. Lim, P. See, J. Lum, X.-M. Zhang, S. Foo, S. Nakamizo, K. Duan, W. T. Kong, R. Gentek, A. Balachander, D. Carabajo, C. Blieriot, B. Malleret, J. K. C. Tam, S. Baig, M. Shabeer, S.-A. E. S. Toh, A. Schlitzer, A. Larbi, T. Marichal, B. Malissen, J. Chen, M. Poidinger, K. Kabashima, M. Bajenoff, L. G. Ng, V. Angeli, F. Ginhoux, Two distinct interstitial macrophage populations coexist across tissues in specific subtissular niches. *Science* **363**, eaau0964 (2019).
5. D. Aran, A. P. Looney, L. Liu, E. Wu, V. Fong, A. Hsu, S. Chak, R. P. Naikawadi, P. J. Wolters, A. R. Abate, A. J. Butte, M. Bhattacharya, Reference-based analysis of lung single-cell sequencing reveals a transitional profibrotic macrophage. *Nat. Immunol.* **20**, 163–172 (2019).
6. M. H. Kaplan, M. M. Hufford, M. R. Olson, The development and in vivo function of T helper 9 cells. *Nat. Rev. Immunol.* **15**, 295–307 (2015).
7. Y. Kimura, T. Takeshita, M. Kondo, N. Ishii, M. Nakamura, J. Van Snick, K. Sugamura, Sharing of the IL-2 receptor  $\gamma$  chain with the functional IL-9 receptor complex. *Int. Immunol.* **7**, 115–120 (1995).
8. S. M. Russell, J. A. Johnston, M. Noguchi, M. Kawamura, C. M. Bacon, M. Friedmann, M. Berg, D. W. McVicar, B. A. Withuhn, O. Silvennoinen, A. S. Goldman, F. C. Schmalstieg, J. N. Ihle, J. J. O'Shea, W. J. Leonard, Interaction of IL-2R $\beta$  and  $\gamma_c$  chains with Jak1 and Jak3: Implications for XSCID and XCID. *Science* **266**, 1042–1045 (1994).
9. S. Takatsuka, H. Yamada, K. Haniuda, H. Saruwatari, M. Ichihashi, J.-C. Renaud, D. Kitamura, IL-9 receptor signaling in memory B cells regulates humoral recall responses. *Nat. Immunol.* **19**, 1025–1034 (2018).
10. A. E. Price, H. E. Liang, B. M. Sullivan, R. L. Reinhardt, C. J. Eisley, D. J. Erle, R. M. Locksley, Systemically dispersed innate IL-13-expressing cells in type 2 immunity. *Proc. Natl. Acad. Sci. U.S.A.* **107**, 11489–11494 (2010).
11. C. Wilhelm, K. Hirota, B. Stieglitz, J. Van Snick, M. Tolaini, K. Lahli, T. Sparwasser, H. Helmby, B. Stockinger, An IL-9 fate reporter demonstrates the induction of an innate IL-9 response in lung inflammation. *Nat. Immunol.* **12**, 1071–1077 (2011).

12. E. C. Nowak, C. T. Weaver, H. Turner, S. Begum-Haque, B. Becher, B. Schreiner, A. J. Coyle, L. H. Kasper, R. J. Noelle, IL-9 as a mediator of Th17-driven inflammatory disease. *J. Exp. Med.* **206**, 1653–1660 (2009).
13. W. Elyaman, E. M. Bradshaw, C. Uyttenhove, V. Dardalhon, A. Awasthi, J. Imitola, E. Bettelli, M. Oukka, J. van Snick, J. C. Renaud, V. K. Kuchroo, S. J. Khouri, IL-9 induces differentiation of  $T_{H}17$  cells and enhances function of FoxP3 $^{+}$  natural regulatory T cells. *Proc. Natl. Acad. Sci. U.S.A.* **106**, 12885–12890 (2009).
14. Y. Wang, J. Shi, J. Yan, Z. Xiao, X. Hou, P. Lu, S. Hou, T. Mao, W. Liu, Y. Ma, L. Zhang, X. Yang, H. Qi, Germinal-center development of memory B cells driven by IL-9 from follicular helper T cells. *Nat. Immunol.* **18**, 921–930 (2017).
15. S. Sehra, W. Yao, E. T. Nguyen, N. L. Glosson-Byers, N. Akhtar, B. Zhou, M. H. Kaplan,  $T_{H}9$  cells are required for tissue mast cell accumulation during allergic inflammation. *J. Allergy Clin. Immunol.* **136**, 433–440.e1 (2015).
16. E. Wambre, V. Bajzik, J. H. DeLong, K. O'Brien, Q. A. Nguyen, C. Speake, V. H. Gersuk, H. A. DeBerg, E. Whalen, C. Ni, M. Farrington, D. Jeong, D. Robinson, P. S. Linsley, B. P. Vickery, W. W. Kwok, A phenotypically and functionally distinct human  $T_{H}2$  cell subpopulation is associated with allergic disorders. *Sci. Transl. Med.* **9**, eaam9171 (2017).
17. A. Shimbara, P. Christodoulopoulos, A. Soussi-Gounni, R. Olivenstein, Y. Nakamura, R. C. Levitt, N. C. Nicolaides, K. J. Holroyd, A. Tsicopoulos, J. J. Lafitte, B. Wallaert, Q. A. Hamid, IL-9 and its receptor in allergic and nonallergic lung disease: Increased expression in asthma. *J. Allergy Clin. Immunol.* **105**, 108–115 (2000).
18. J. Kearley, J. S. Erjefalt, C. Andersson, E. Benjamin, C. P. Jones, A. Robichaud, S. Pegorier, Y. Brewah, T. J. Burwell, L. Bjermer, P. A. Kiener, R. Kolbeck, C. M. Lloyd, A. J. Coyle, A. A. Humbles, IL-9 governs allergen-induced mast cell numbers in the lung and chronic remodeling of the airways. *Am. J. Respir. Crit. Care Med.* **183**, 865–875 (2011).
19. P. Kauppi, T. Laitinen, V. Ollikainen, H. Mannila, L. A. Laitinen, J. Kere, The IL9R region contribution in asthma is supported by genetic association in an isolated population. *Eur. J. Hum. Genet.* **8**, 788–792 (2000).
20. C. Pilette, Y. Ouadrihiri, J. Van Snick, J.-C. Renaud, P. Staquet, J.-P. Vaerman, Y. Sibille, Oxidative burst in lipopolysaccharide-activated human alveolar macrophages is inhibited by interleukin-9. *Eur. Respir. J.* **20**, 1198–1205 (2002).
21. C. Pilette, Y. Ouadrihiri, J. Van Snick, J. C. Renaud, P. Staquet, J. P. Vaerman, Y. Sibille, IL-9 inhibits oxidative burst and TNF- $\alpha$  release in lipopolysaccharide-stimulated human monocytes through TGF- $\beta$ . *J. Immunol.* **168**, 4103–4111 (2002).
22. J.-A. Gonzalo, C. M. Lloyd, D. Wen, J. P. Albar, T. N. C. Wells, A. Proudfoot, C. Martinez-A, M. Dorf, T. Bjerke, A. J. Coyle, J.-C. Gutierrez-Ramos, The coordinated action of CC chemokines in the lung orchestrates allergic inflammation and airway hyperresponsiveness. *J. Exp. Med.* **188**, 157–167 (1998).
23. A. V. Misharin, L. Morales-Nebreda, P. A. Reyfman, C. M. Cuda, J. M. Walter, A. C. McQuattie-Pimentel, C. I. Chen, K. R. Anekalla, N. Joshi, K. J. N. Williams, H. Abdala-Valencia, T. J. Yacoub, M. Chi, S. Chiu, F. J. Gonzalez-Gonzalez, K. Gates, A. P. Lam, T. T. Nicholson, P. J. Homan, S. Soberanes, S. Dominguez, V. K. Morgan, R. Saber, A. Shaffer, M. Hinckcliff, S. A. Marshall, A. Bharat, S. Berdnikovs, S. M. Bhorade, E. T. Bartom, R. I. Morimoto, W. E. Balch, J. I. Szajnader, N. S. Chandel, G. M. Mutlu, M. Jain, C. J. Gottardi, B. D. Singer, K. M. Ridge, N. Bagheri, A. Shilatifard, G. R. S. Budinger, H. Perlman, Monocyte-derived alveolar macrophages drive lung fibrosis and persist in the lung over the life span. *J. Exp. Med.* **214**, 2387–2404 (2017).
24. H. Cui, D. Jiang, S. Banerjee, N. Xie, T. Kulkarni, R. M. Liu, S. R. Duncan, G. Liu, Monocyte-derived alveolar macrophage apolipoprotein E participates in pulmonary fibrosis resolution. *JCI Insight* **5**, (2020).
25. P. P. Ogger, G. J. Albers, R. J. Hewitt, B. J. O'Sullivan, J. E. Powell, E. Calamita, P. Ghai, S. A. Walker, P. McErlean, P. Saunders, S. Kingston, P. L. Molyneaux, J. M. Halket, R. Gray, D. C. Chambers, T. M. Maher, C. M. Lloyd, A. J. Byrne, Itaconate controls the severity of pulmonary fibrosis. *Sci. Immunol.* **5**, eabc1884 (2020).
26. S. Takatsuka, H. Yamada, K. Haniuda, M. Ichihashi, J. Chiba, D. Kitamura, DNA immunization using *in vivo* electroporation for generating monoclonal antibodies against mouse IL-9R. *Bio Protoc.* **9**, e3174 (2019).
27. L. Huang, E. V. Nazarova, S. Tan, Y. Liu, D. G. Russell, Growth of *Mycobacterium tuberculosis* *in vivo* segregates with host macrophage metabolism and ontogeny. *J. Exp. Med.* **215**, 1135–1152 (2018).
28. Z. Zasłona, S. Przybranowski, C. Wilke, N. van Rooijen, S. Teitz-Tennenbaum, J. J. Osterholzer, J. E. Wilkinson, B. B. Moore, M. Peters-Golden, Resident alveolar macrophages suppress, whereas recruited monocytes promote, allergic lung inflammation in murine models of asthma. *J. Immunol.* **193**, 4245–4253 (2014).
29. W. Yao, Y. Zhang, R. Jabeen, E. T. Nguyen, D. S. Wilkes, R. S. Tepper, M. H. Kaplan, B. Zhou, Interleukin-9 is required for allergic airway inflammation mediated by the cytokine TSLP. *Immunity* **38**, 360–372 (2013).
30. R. S. Tepper, C. J. Llapur, M. H. Jones, C. Tiller, C. Coates, R. Kimmel, J. Kisling, B. Katz, Y. Ding, N. Swigonski, Expired nitric oxide and airway reactivity in infants at risk for asthma. *J. Allergy Clin. Immunol.* **122**, 760–765 (2008).
31. W. Yao, F. M. Barbé-Tuana, C. J. Llapur, M. H. Jones, C. Tiller, R. Kimmel, J. Kisling, E. T. Nguyen, J. Nguyen, Z. Yu, M. H. Kaplan, R. S. Tepper, Evaluation of airway reactivity and immune characteristics as risk factors for wheezing early in life. *J. Allergy Clin. Immunol.* **126**, 483–488.e1 (2010).
32. F. Tacke, F. Ginhoux, C. Jakubzick, N. van Rooijen, M. Merad, G. J. Randolph, Immature monocytes acquire antigens from other cells in the bone marrow and present them to T cells after maturing in the periphery. *J. Exp. Med.* **203**, 583–597 (2006).
33. A. A. Litonjua, J. Lasky-Su, K. Schneiter, K. G. Tantisira, R. Lazarus, B. Klanderman, J. J. Lima, C. G. Irvin, S. P. Peters, J. P. Hanrahan, S. B. Liggett, G. A. Hawkins, D. A. Meyers, E. R. Bleeker, C. Lange, S. T. Weiss, ARG1 is a novel bronchodilator response gene: Screening and replication in four asthma cohorts. *Am. J. Respir. Crit. Care Med.* **178**, 688–694 (2008).
34. L. A. Monticelli, M. D. Buck, A. L. Flamar, S. A. Saenz, E. D. Tait Wojno, N. A. Yudanin, L. C. Osborne, M. R. Hepworth, S. V. Tran, H. R. Rodewald, H. Shah, J. R. Cross, J. M. Diamond, E. Cantu, J. D. Christie, E. L. Pearce, D. Artis, Arginase 1 is an innate lymphoid-cell-intrinsic metabolic checkpoint controlling type 2 inflammation. *Nat. Immunol.* **17**, 656–665 (2016).
35. E. E. Sarria, R. Mattiello, W. Yao, V. Chakr, C. J. Tiller, J. Kisling, R. Tabbey, Z. Yu, M. H. Kaplan, R. S. Tepper, Atopy, cytokine production, and airway reactivity as predictors of pre-school asthma and airway responsiveness. *Pediatr. Pulmonol.* **49**, 132–139 (2014).
36. T. A. Wynn, K. M. Vannella, Macrophages in tissue repair, regeneration, and fibrosis. *Immunity* **44**, 450–462 (2016).
37. J. Schyns, Q. Bai, C. Ruscitti, C. Radermecker, S. De Schepper, S. Chakarov, F. Farnir, D. Pirottin, F. Ginhoux, G. Boeckstaens, F. Bureau, T. Marichal, Non-classical tissue monocytes and two functionally distinct populations of interstitial macrophages populate the mouse lung. *Nat. Commun.* **10**, 3964 (2019).
38. B. B. Ural, S. T. Yeung, P. Damani-Yokota, J. C. Devlin, M. de Vries, P. Vera-Licona, T. Samji, C. M. Sawai, G. Jang, O. A. Perez, Q. Pham, L. Maher, P. Loke, M. Dittmann, B. Reizis, K. M. Khanna, Identification of a nerve-associated, lung-resident interstitial macrophage subset with distinct localization and immunoregulatory properties. *Sci. Immunol.* **5**, eaax8756 (2020).
39. G. Donniniell, I. Saraf-Sinik, V. Mazzotti, A. Capone, M. G. Grasso, L. Battistini, R. Reynolds, R. Magliozzi, E. Volpe, Interleukin-9 regulates macrophage activation in the progressive multiple sclerosis brain. *J. Neuroinflammation* **17**, 149 (2020).
40. J. F. Lai, L. J. Thompson, S. F. Ziegler, TSLP drives acute  $T_{H}2$ -cell differentiation in lungs. *J. Allergy Clin. Immunol.* **146**, 1406–1418.e7 (2020).
41. P. J. Murray, Macrophage polarization. *Annu. Rev. Physiol.* **79**, 541–566 (2017).
42. R. H. Cloots, S. Sankaranarayanan, C. C. de Theije, M. E. Poynter, E. Terwindt, P. van Dijk, T. B. Hakvoort, W. H. Lamers, S. E. Köhler, Ablation of Arg1 in hematopoietic cells improves respiratory function of lung parenchyma, but not that of larger airways or inflammation in asthmatic mice. *Am. J. Physiol. Lung Cell. Mol. Physiol.* **305**, L364–L376 (2013).
43. R. H. E. Cloots, M. E. Poynter, E. Terwindt, W. H. Lamers, S. E. Köhler, Hypoargininemia exacerbates airway hyperresponsiveness in a mouse model of asthma. *Respir. Res.* **19**, 98 (2018).
44. R. H. E. Cloots, S. Sankaranarayanan, M. E. Poynter, E. Terwindt, P. van Dijk, W. H. Lamers, S. Eleonore Köhler, Arginase 1 deletion in myeloid cells affects the inflammatory response in allergic asthma, but not lung mechanics, in female mice. *BMC Pulm. Med.* **17**, 158 (2017).
45. K. A. Niese, A. R. Collier, A. R. Hajek, S. D. Cederbaum, W. E. O'Brien, M. Wills-Karp, M. E. Rothenberg, N. Zimmermann, Bone marrow cell derived arginase I is the major source of allergen-induced lung arginase but is not required for airway hyperresponsiveness, remodeling and lung inflammatory responses in mice. *BMC Immunol.* **10**, 33 (2009).
46. H. Maarsingh, B. G. Dekkers, A. B. Zuidhof, I. S. Bos, M. H. Menzen, T. Klein, G. Flik, J. Zaagsma, H. Meurs, Increased arginase activity contributes to airway remodelling in chronic allergic asthma. *Eur. Respir. J.* **38**, 318–328 (2011).
47. H. Maarsingh, A. B. Zuidhof, I. S. Bos, M. van Duin, J. L. Boucher, J. Zaagsma, H. Meurs, Arginase inhibition protects against allergen-induced airway obstruction, hyperresponsiveness, and inflammation. *Am. J. Respir. Crit. Care Med.* **178**, 565–573 (2008).
48. M. L. North, N. Khanna, P. A. Marsden, H. Grasemann, J. A. Scott, Functionally important role for arginase 1 in the airway hyperresponsiveness of asthma. *Am. J. Physiol. Lung Cell. Mol. Physiol.* **296**, L911–L920 (2009).
49. M. Yang, D. Rangasamy, K. I. Matthaei, A. J. Frew, N. Zimmermann, S. Mahalingam, D. C. Webb, D. J. Tremethick, P. J. Thompson, S. P. Hogan, M. E. Rothenberg, W. B. Cowden, P. S. Foster, Inhibition of arginase I activity by RNA interference attenuates IL-13-induced airways hyperresponsiveness. *J. Immunol.* **177**, 5595–5603 (2006).
50. N. Zimmermann, N. E. King, J. Laporte, M. Yang, A. Mishra, S. M. Pope, E. E. Munzel, D. P. Witte, A. A. Pegg, P. S. Foster, Q. Hamid, M. E. Rothenberg, Dissection

- of experimental asthma with DNA microarray analysis identifies arginase in asthma pathogenesis. *J. Clin. Invest.* **111**, 1863–1874 (2003).
51. L. Barron, A. M. Smith, K. C. El Kasmi, J. E. Qualls, X. Huang, A. Cheever, L. A. Borthwick, M. S. Wilson, P. J. Murray, T. A. Wynn, Role of arginase 1 from myeloid cells in th2-dominated lung inflammation. *PLOS ONE* **8**, e61961 (2013).
  52. D. R. Herbert, T. Orekov, A. Roloson, M. Ilies, C. Perkins, W. O'Brien, S. Cederbaum, D. W. Christianson, N. Zimmermann, M. E. Rothenberg, F. D. Finkelman, Arginase I suppresses IL-12/IL-23p40-driven intestinal inflammation during acute schistosomiasis. *J. Immunol.* **184**, 6438–6446 (2010).
  53. J. T. Pesce, T. R. Ramalingam, M. M. Mentink-Kane, M. S. Wilson, K. C. El Kasmi, A. M. Smith, R. W. Thompson, A. W. Cheever, P. J. Murray, T. A. Wynn, Arginase-1-expressing macrophages suppress Th2 cytokine-driven inflammation and fibrosis. *PLOS Pathog.* **5**, e1000371 (2009).
  54. J. E. Turner, P. J. Morrison, C. Wilhelm, M. Wilson, H. Ahlfors, J. C. Renauld, U. Panzer, H. Helmby, B. Stockinger, IL-9-mediated survival of type 2 innate lymphoid cells promotes damage control in helminth-induced lung inflammation. *J. Exp. Med.* **210**, 2951–2965 (2013).
  55. J. Venge, M. Lampinen, L. Häkansson, S. Rak, P. Venge, Identification of IL-5 and RANTES as the major eosinophil chemoattractants in the asthmatic lung. *J. Allergy Clin. Immunol.* **97**, 1110–1115 (1996).
  56. R. E. Marques, R. Guabiraba, R. C. Russo, M. M. Teixeira, Targeting CCL5 in inflammation. *Expert Opin. Ther. Targets* **17**, 1439–1460 (2013).
  57. T. A. Reese, H.-E. Liang, A. M. Tager, A. D. Luster, N. Van Rooijen, D. Voehringer, R. M. Locksley, Chitin induces accumulation in tissue of innate immune cells associated with allergy. *Nature* **447**, 92–96 (2007).
  58. V. Steenwinckel, J. Louahed, C. Orabona, F. Huaux, G. Warnier, A. McKenzie, D. Lison, R. Levitt, J.-C. Renaud, IL-13 mediates in vivo IL-9 activities on lung epithelial cells but not on hematopoietic cells. *J. Immunol.* **178**, 3244–3251 (2007).
  59. M. J. Townsend, P. G. Fallon, D. J. Matthews, P. Smith, H. E. Jolin, A. N. J. McKenzie, IL-9-deficient mice establish fundamental roles for IL-9 in pulmonary mastocytosis and goblet cell hyperplasia but not T cell development. *Immunity* **13**, 573–583 (2000).
  60. D. Chang, W. Yao, C. J. Tiller, J. Kisling, J. E. Slaven, Z. Yu, M. H. Kaplan, R. S. Tepper, Exhaled nitric oxide during infancy as a risk factor for asthma and airway hyperreactivity. *Eur. Respir. J.* **45**, 98–106 (2015).
  61. M. Stoeckius, C. Hafemeister, W. Stephenson, B. Houck-Loomis, P. K. Chattopadhyay, H. Swerdlow, R. Satija, P. Smibert, Simultaneous epitope and transcriptome measurement in single cells. *Nat. Methods* **14**, 865–868 (2017).
  62. M. Stoeckius, S. Zheng, B. Houck-Loomis, S. Hao, B. Z. Yeung, W. M. Mauck III, P. Smibert, R. Satija, Cell hashing with barcoded antibodies enables multiplexing and doublet detection for single cell genomics. *Genome Biol.* **19**, 224 (2018).
  63. A. Butler, P. Hoffman, P. Smibert, E. Papalexi, R. Satija, Integrating single-cell transcriptomic data across different conditions, technologies, and species. *Nat. Biotechnol.* **36**, 411–420 (2018).
  64. T. Stuart, A. Butler, P. Hoffman, C. Hafemeister, E. Papalexi, W. M. Mauck III, Y. Hao, M. Stoeckius, P. Smibert, R. Satija, Comprehensive integration of single-cell data. *Cell* **177**, 1888–1902.e21 (2019).

**Acknowledgments:** We thank H. Serezani for review of this manuscript. We thank the members of the Indiana University Melvin and Bren Simon Cancer Center Flow Cytometry Resource Facility for outstanding technical support. Schematics in Fig. 3 were generated with BioRender.com. **Funding:** This work was supported by Public Health Service grants from the National Institutes of Health (R01 AI129241 to M.H.K.). B.Z. was supported by Public Health Service grants from the National Institutes of Health (R01 AI085046). B.J.U. was supported by National Institutes of Health grants T32 AI060519 and F30 HL147515. A.P. was supported by National Institutes of Health grant T32 AI060519. J.S. was supported by Public Health Service grants from the National Institutes of Health (AG069264 and AI147394). The Indiana University Melvin and Bren Simon Comprehensive Cancer Center Flow Cytometry Resource Facility were supported, in part, by NIH, National Cancer Institute (NCI) grant P30 CA082709 and National Institute of Diabetes and Digestive and Kidney Diseases (NIDDK) grant U54 DK106846. The Flow Cytometry Resource Facility was supported, in part, by NIH instrumentation grant 1S10D012270. Support provided by the Herman B Wells Center for Pediatric Research was, in part, from the Riley Children's Foundation. **Author contributions:** Y.F. and M.H.K. designed the experiments. Y.F. performed the experiments and analyzed the data. H.G. and Y.F. performed the bioinformatic experiments and analysis. J.W., B.Z., B.R., B.K., B.J.U., S.Y., and A.P. assisted with the experiments. R.K., J.-C.R., S.P., Y.L., R.M.T., P.L.-L., R.A.F., S.T., D.K., R.S.T., and J.S. provided reagents, mice, and advice. Y.F. and M.H.K. coordinated the project and wrote the manuscript with input from all the authors. **Competing interests:** The authors declare that they have no competing interests. R.A.F. is an advisor to Glaxo Smith Kline, Zai Lab, and Ventus Therapeutics. **Data and materials availability:** CITE-seq data are available under GEO accession number GSE162898. All data needed to evaluate the conclusions in the paper are present in the paper or the Supplementary Materials. *Il9r<sup>-/-</sup>* mice are available from J.-C.R. under a material transfer agreement with the Ludwig Institute for Cancer Research Ltd. The anti-IL-9R monoclonal antibody (mAb) was initially obtained from D.K. under a material transfer agreement with Tokyo University of Science. The anti-IL-9R mAb is now commercially available.

Submitted 13 April 2021

Accepted 27 January 2022

Published 18 February 2022

10.1126/scimmunol.abi9768

## An IL-9–pulmonary macrophage axis defines the allergic lung inflammatory environment

Yongyao FuJocelyn WangBaohua ZhouAbigail PajulasHongyu GaoBaskar RamdasByunghee KohBenjamin J. UlrichShuangshuang YangReuben KapurJean-Christophe RenauldSophie PaczesnyYunlong LiuRobert M. TighePaula Licona-LimónRichard A. FlavellShogo TakatsukaDaisuke KitamuraRobert S. TepperJie SunMark H. Kaplan

*Sci. Immunol.*, 7 (68), eabi9768. • DOI: 10.1126/sciimmunol.abi9768

### Macrophages amplify allergic airway inflammation

Interleukin-9 (IL-9) can promote type 2 lung inflammation during allergic responses to inhaled allergens, but the direct cellular targets of IL-9 are not well characterized. Fu *et al.* demonstrate that pulmonary macrophages are a major population of immune cells responding to IL-9 produced in mouse models of allergic airway disease. Mice deficient in the IL-9 receptor had impaired expansion of monocyte-derived interstitial macrophages that promoted airway inflammation dependent on arginase expression. IL-9 signaling also promoted macrophage production of the eosinophil-attracting chemokine CCL5, which was elevated in the serum of patients with asthma and correlated with IL-9 levels. These results identify lung macrophages as key cellular targets of IL-9 during allergic disease that subsequently amplify type 2 inflammatory responses.

### View the article online

<https://www.science.org/doi/10.1126/sciimmunol.abi9768>

### Permissions

<https://www.science.org/help/reprints-and-permissions>